AUTOMATIC DETECTION OF NYSTAGMUS IN BEDSIDE VOG RECORDINGS FROM PATIENTS WITH VERTIGO

by

Sai Akanksha Punuganti

A thesis submitted to Johns Hopkins University in conformity with the requirements for the degree of Master of Science in Engineering

Baltimore, Maryland

August, 2019

© 2019 Sai Akanksha Punuganti

All rights reserved

Abstract

Benign Paroxysmal Positional Vertigo (BPPV) is the most common cause of vertigo. It can be diagnosed and treated using simple maneuvers done by vestibular experts. However, patients with this condition presenting to the emergency department have high chance of being misdiagnosed. Such high rate of misdiagnosis results in significant morbidity to the patient and also incurs huge medical costs from unnecessary neuroimaging tests. Hence, automatic medical diagnosis is the next step to aid ED practitioners to reduce diagnostic errors. However, current software employed for this diagnosis has been found to have very low specificity. This can be attributed to factors such as low sampling frequency of recording device and the fact that bedside recordings from patients are susceptible to noise and artifacts. This study aims to improve methods for automatic quantification of nystagmus, a key sign of BPPV. Testing the current method using eye movement data recorded in patients during the diagnostic maneuver yielded better results than the commercial software.

Thesis Committee

Primary Readers

Jorge Otero-Millan (Primary Advisor)
Post-doctoral Fellow
Department of Neurology
Johns Hopkins School of Medicine

Michael Schubert
Associate Professor
Department of Otolaryngology - Head and Neck Surgery
Johns Hopkins School of Medicine

Kathleen Cullen
Professor
Department of Biomedical Engineering
Johns Hopkins University, Whiting School of Engineering

Amir Kheradmand (Thesis Committee Chair)
Assistant Professor
Department of Neurology
Johns Hopkins School of Medicine

Acknowledgments

I'd like to express my immense gratitude to **Dr. Jorge Otero-Millan**. Thank you for always being there for me. Your knowledge, patience, humor and tenacity are a huge source of inspiration to me. I'm very much grateful to have you as my advisor and mentor, your unwavering support and encouragement is hard to find. Thank you for giving me the opportunity to work with you.

I'd like to thank **Dr. Amir Kheradmand** for believing in me and giving me my first chance to work at VORlab. You've provided me with a lifelong platform that I hope to always treasure. Your mentoring is truly valuable to me, thank you. **Dr. Jing Tian**, thank you for being you. Your patience, guidance and advice have helped me steer on the right path.

Dr. David Zee, Dr. Shirin Sadeghpour, Dr. Ari Shemesh, Dr. Jacob Pogson, and Rebecca Scholz - Thank you all for creating an amazing lab atmosphere. Your deeds and words are a source of motivation, I'll always cherish them. **Samuel Bourne** and **Ayodele McClenney**, thank you for your valuable advice and patient guidance. Lastly, I'd like to thank **Dr. Madhusudhan Rao** for his generous heart and rigorous training.

I feel grateful to have had the opportunity to work in this lab. I've been nurtured and inspired in ways that is only possible by this lab. Thank you all.

Dedication

This thesis is dedicated to my family, without whose endless support and love I'd not be able to take my risks and find myself.

Table of Contents

List of Tables

List of Figures

List of Acronyms

AUC Area Under Curve. 57, 72

BIT Binocular-Individual Threshold. 20, 26, 28

BLSTM Bidirectional Long Short-Term Memory. 22, 23, 27, 28

BMD Bayesian Microsaccade Detection. 21, 27, 28

BMM Bayesian Mixture Model. 27

BPPV Benign Paroxysmal Positional Vertigo. 2, 3, 8, 10, 12, 14, 17, 26, 58, 68, 69

CDT Identification by analysis of Variance and Covariance. 20, 21, 27, 28

CNN Convolutional Neural Network. 22, 23, 27, 28, 70

CSV Comma Separated Values. 30, 33

ED Emergency Department. 1–3, 68

EK Algorithm by Engbert and Mergenthaler, 2006. 20, 21, 26, 28

EM-GMM Expectation Maximization (EM) Algorithm for Gaussian Mixture Model. 27

EMG Electromyography. 11, 12

ENG Electronystagmography. 11, 25

EOG Electro Oculography. 13, 14

FIR Finite Impulse Response. 25

HC Hooge and Clamp Adaptive Velocity Threshold Algorithm. 20, 26, 28

I2MC Identification by Two-Means Clustering. 19, 20, 27, 28

IAOI Identification by Area-Of-Interest. 18, 19, 26, 28

IBDT Identification by Bayesian Decision Theory. 23, 27, 28

IDT Identification by Dispersion Threshold. 18, 19, 26, 28

IHMM Identification by Hidden Markov Model. 18–20, 27, 28

IIR Infinite Impulse Response. 25

IKF Identification by Kalman Filter. 19, 20, 27, 28

IMSF Identification by Membership Function. 26

IMST Identification by Minimum Spanning Tree. 18–20, 27, 28

IPF Identification by Particle Filter. 21, 27

IRF Identification by Random Forest. 19, 23, 27, 28

IVDT Identification by Velocity and Dispersion Threshold. 22, 23, 26, 28

IVMP Identification by Velocity and Movement Pattern. 22, 26, 28

IVT Identification by Velocity Threshold. 18, 19, 26, 28

IVVT Modified version of IVT Algorithm. 22, 26, 28

LED Light Emitting Diodes. 15

LNS Algorithm by Larsson, Nyström and Stridh, 2013. 20, 23, 26, 28

LNS15 Algorithm proposed by Larsson et al., 2015. 28

LNS16 Algorithm proposed by Larsson et al., 2016. 28

MAD Median Absolute Deviation. 53, 77

MBSDC Model-based Separation, Detection, and Classification. 23, 27, 28

MDS Multi-Dimensional Scaling. xiv, 50, 51

NH Adaptive Velocity algorithm. 19, 20, 26, 28

NN Neural Network. 22, 24

NPV Negative Predictive Value. 63–66, 69

NSLR-HMM Naive Segmented Linear Regression based Hidden Markov Model. 20, 26, 28

OKN Optokinetic Nystagmus. 24

OM K-Means Algorithm by Otero-Milan et al., 2014. 21, 27, 28

PPV Positive Predictive Value. 63–66, 69

PSO Post-Saccadic Oscillation. 23

QPs Quick Phases. xiv, 45, 50, 51, 54, 68

REMoDNaV Robust Eye Movement Detection for Natural Viewing. 20, 23, 26, 28

RNN Recurrent Neural Network. 22

ROC Receiver Operating Characteristic. viii, xiv, 55–60, 69, 72

SLO Scanning Laser Ophthalmoscope. 13

SPV Slow Phase Velocity. xiii, xiv, 10, 17, 30, 31, 36–38, 44, 46, 52, 53, 55, 56, 59–62, 67, 69, 72, 75

SVM Support Vector Machine. 27

SVV Subjective Visual Vertical. 12

VEMPs Vestibular Evoked Myogenic Potentials. 11

VFTs Vestibular Function Tests. 11, 12, 30

vHIT Video Head Impulse Test. 11, 30

VOG Video Oculography. xii, xiii, 2, 3, 10–14, 16, 22, 25, 29, 32, 33, 41, 42, 68, 72

VOR Vestibulo-Ocular Reflex. 7, 11, 24, 42

WSJ Identification by Velocity Threshold for low- and high- noise data. 20, 26, 28

XML eXtensible Markup Language. 30, 31

Chapter 1

Introduction

1.1 Motivation

About 3.3% of chief complaints in hospital emergency departments pertain to dizziness and vertigo (Newman-Toker et al., 2008). They can be caused either by a dangerous brain injury (like stroke) or a benign ear problem (vestibular vertigo). Clinicians in the ED mostly rely on general neurological tests to identify central signs which makes it challenging to differentiate central disorders from benign peripheral vestibulopathies (Newman-Toker, 2016). Further, the rate of misdiagnosis is high, considering the fact that only 19% of dizzy-stroke patients have focal neurological signs (Kattah Jorge C. et al., 2009). Although there exists an accurate bedside test (HINTS: Head Impulse, Nystagmus and Test of Skew) to distinguish diagnosis of stroke in patients with acute vestibular syndrome, most ED physicians are not familiar with this test. Hence, automatic medical diagnosis for such patients has the potential to mitigate the existing high rate of misdiagnosis by aiding to distinguish between the different causes.

Benign Paroxysmal Positional Vertigo (BPPV) is the most common cause of vertigo and dizziness. This condition can be treated and diagnosed using simple positional tests. Patients suffering from BPPV present vestibular **nystagmus** during diagnostic maneuvers such as the Dix-Hallpike (Dix and Hallpike, 1952) or the Rolling Maneuver (Lanska and Remler, 1997).

Nystagmus can be described as an involuntary and repeated eye movement pattern. It comprises of alternating slow eye drifts in one direction (slow phases) and rapid saccades in the opposite direction (quick phases). Estimation of velocity of eye during slow phases is crucial for the quantification of the intensity of the vestibular nystagmus (also called as jerk nystagmus). Currently, the vestibular diagnostic tests are conducted at bedside, with the patient wearing an eye tracker (Video Oculography (VOG) goggles) and vision denied. Hence the readings are also prone to head movement artifacts apart from general ones like noise, blinks, loss of pupil center etc., which pose further challenges towards automatic detection of nystagmus.

1.2 Problem Statement

Benign Paroxysmal Positional Vertigo (BPPV) is the most common cause of vertigo and dizziness. It can be treated as well as diagnosed using simple maneuvers done by specialists orienting the patient's head into prescribed positions. However, dizzy patients visiting the ED have **43%** chances of being misdiagnosed (Brevern et al., 2006).

Employing automatic medical diagnosis could aid ED practitioners in making better diagnosis, or even helping patients with self diagnosis. Eye

movement recordings are a crucial aspect to achieve this automatic diagnosis, especially to aid in automatic detection of nystagmus. One of the most common software and devices used to record eye movements during these tests is the ICS Impulse Otosuite (GN Otometrics^{TM}, Taastrup, Denmark) system. However this software is shown to have low specificity in detecting nystagmus. Diagnostic tests having low specificity have higher tendency to classify patients without disease as positive. In other words, the low specificity of the software leads to higher false positive cases, creating the need for careful expert reviewing in each positive case.

The present study explores a method for automatic detection of nystagmus as a result of BPPV for point-of-care diagnosis in the ED. This paper also serves to validate one of the most common VOG software and devices employed by clinicians in the detection of nystagmus, ICS Impulse Otosuite (GN Otometrics^{TM}, Taastrup, Denmark). Due to the low quality nature of bedside data recordings from the ED, the current detection algorithm must be robust to bad data and artifacts in order to offer high sensitivity and specificity.

1.3 Thesis Overview

The succeeding chapter discusses further background and clinical need for the present study. Chapter 3 on literature review provides an overview of the existing algorithms published in the literature to detect different eye movements, with special focus on detection of saccades. The eye movement data used in present study, its recording, extraction, challenges and other factors characteristic of this data are briefly described in chapter 4. Chapter 5

describes in detail the proposed algorithm for automatic nystagmus detection. Chapter 6 shows the results obtained by using present method. Chapter 7 concludes the dissertation by discussing the custom algorithm and future steps to be done.

Chapter 2

Background

2.1 Physiology

2.1.1 Vertigo and Dizziness

Vertigo can be described as the feeling of spinning or lack of balance while dizziness, a potential symptom of vertigo, can be described as the feeling of lightheadedness. They remain one of the most frequent complaints in medicine, affecting upto 30% of the general population (Hannaford et al., 2005). Affected patients are found to make multiple visits to several specialty physicians ranging from ENT specialists and neurologists to orthopaedists (Strupp and Brandt, 2008). The lifetime prevalence of these conditions is found to be up to 30% (Neuhauser, 2007), with the patient experiencing significant healthcare burden and psychological impact (Neuhauser et al., 2008). Causes for these conditions include dangerous brain injury (like stroke) or benign ear problem (vestibular vertigo). However, the latter is found to be the most common cause, which moreover is deemed to produce considerable burden to the affected patients (Neuhauser et al., 2008).

2.1.2 Vestibular System

Though it is largely believed that humans have only five senses, we are equipped with numerous other senses that are less known. One of them is the vestibular system. The **human vestibular system** allows us to keep our balance and detect the direction and speed of our head movements. It enables us to interact with our environment by informing us about the alignment of our body parts in space. It is located within the human inner ears and comprises of various elements of which the semi-circular canals and the otoliths are among the major ones:

- **Semi-circular canals:** These are tiny, fluid-filled semi-circular tubes in the inner ear (Figure 2.1) that help sense head rotation. There are 3 semi-circular canals within each inner ear, corresponding to the 3D world we live in. The fluid within each of the canals is called endolymph. During head rotation, the endolymph instead of being displaced simultaneously, lags due to its viscous nature. This relative displacement of the endolymph with respect to the canals pushes the hair cells (sensory receptors of the vestibular systems) that then relay the information to oculomotor nuclei of the brainstem, which innervate the eye muscles. The stimulation of the oculomotor nuclei in this way produces eye movements that counteract the direction of head rotation.

- **Otoliths:** These are formed by calcium carbonate crystals held together within a gelatinous matrix attached to the hair cells and help sense linear acceleration of the head (Figure 2.1). Displacement of the head causes

the otoliths to move which in turn push the hair cells. This movement of hair cells is sensed by the brain, thereby enabling us to synthesize information regarding the linear acceleration and the orientation of the head movement in relation to the direction of gravity.

The **Vestibulo-Ocular Reflex (VOR)** provides an example of the influence of the vestibular system (particularly the semi-circular canals and the otoliths) on eye movements. In order to fixate on an object while the head is moving, the image of the object has to remain constant on the retina. The linear and angular acceleration of the head movement are sensed by the canals and otoliths which then relay this information to the oculomotor nuclei. The oculomotor nuceli, after thus being stimulated by the vestibular system, cause the eyes to move opposite to the direction of head movement so that the image of the object is preserved on the retina. This response is termed VOR.

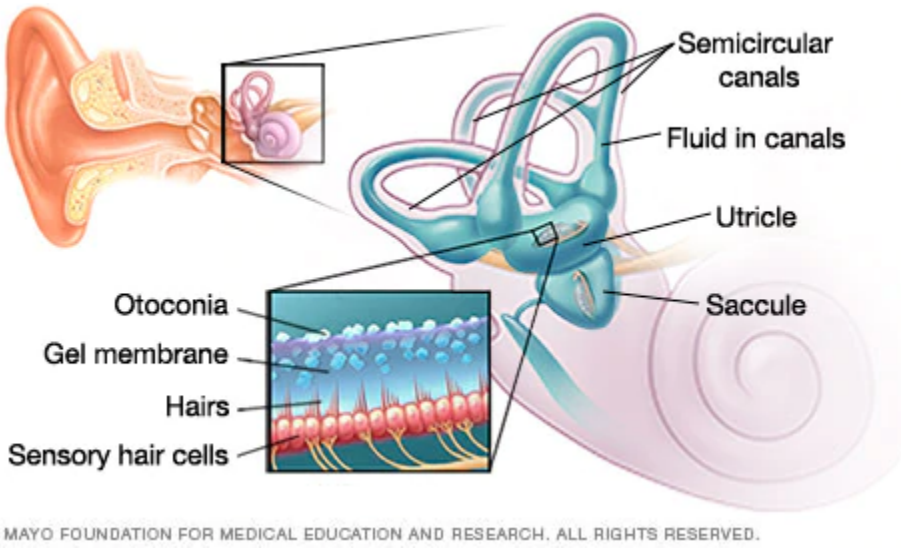

Figure 2.1: Vestibular System Semi-circular canals and the otoliths (Utricle and Saccule) of the vestibular system residing inside the inner ear. Reproduced from *Mayoclinic.org* (2018), *Inner ear and balance*.

2.1.3 Benign Paroxysmal Positional Vertigo

Some of the otolith crystals can get detached from the gelatinous matrix that holds them together due to various reasons ranging from ear infection or other diseases to aging. The detached otoliths often migrate into one of the semi-circular canals where they are suspended in the endolymph. These suspended otoliths are also called **otoconia**. Due to their placement, otoliths are most often seen to migrate to the posterior canal (Parnes, Agrawal, and Atlas, 2003).

Since otoconia are denser than endolymph, their displacement also causes the hair cells to move. The presence of these additional signals from the hair cells causes a disturbance in how the brain interprets rotation of the head, consequently resulting in vertigo and dizziness. This condition is referred to as Benign Paroxysmal Positional Vertigo (BPPV).

BPPV is the most common cause of vertigo (Kim and Zee, 2014). The episodes of vertigo occurring in this condition are brief (less than a minute) and are provoked by specific positions such as when getting in to bed, rolling in bed, getting up suddenly, or looking up (Solomon, 2000).

This condition can be diagnosed and treated with simple maneuvers in which experts orient the patient to prescribed positions. The **Epley maneuver** (Epley, 1980; Hilton and Pinder, 2014) is used to treat this condition which includes expert positioning of the patient's body in specific orientations to guide the otoconia out of the semi circular canals. Similarly, the **Dix Hallpike Maneuver** (Dix and Hallpike, 1952) shown in Figure 2.2 is the gold standard in diagnosis of BPPV. This maneuver includes simple steps done by experts and at the end of it patient shows signs of nystagmus.

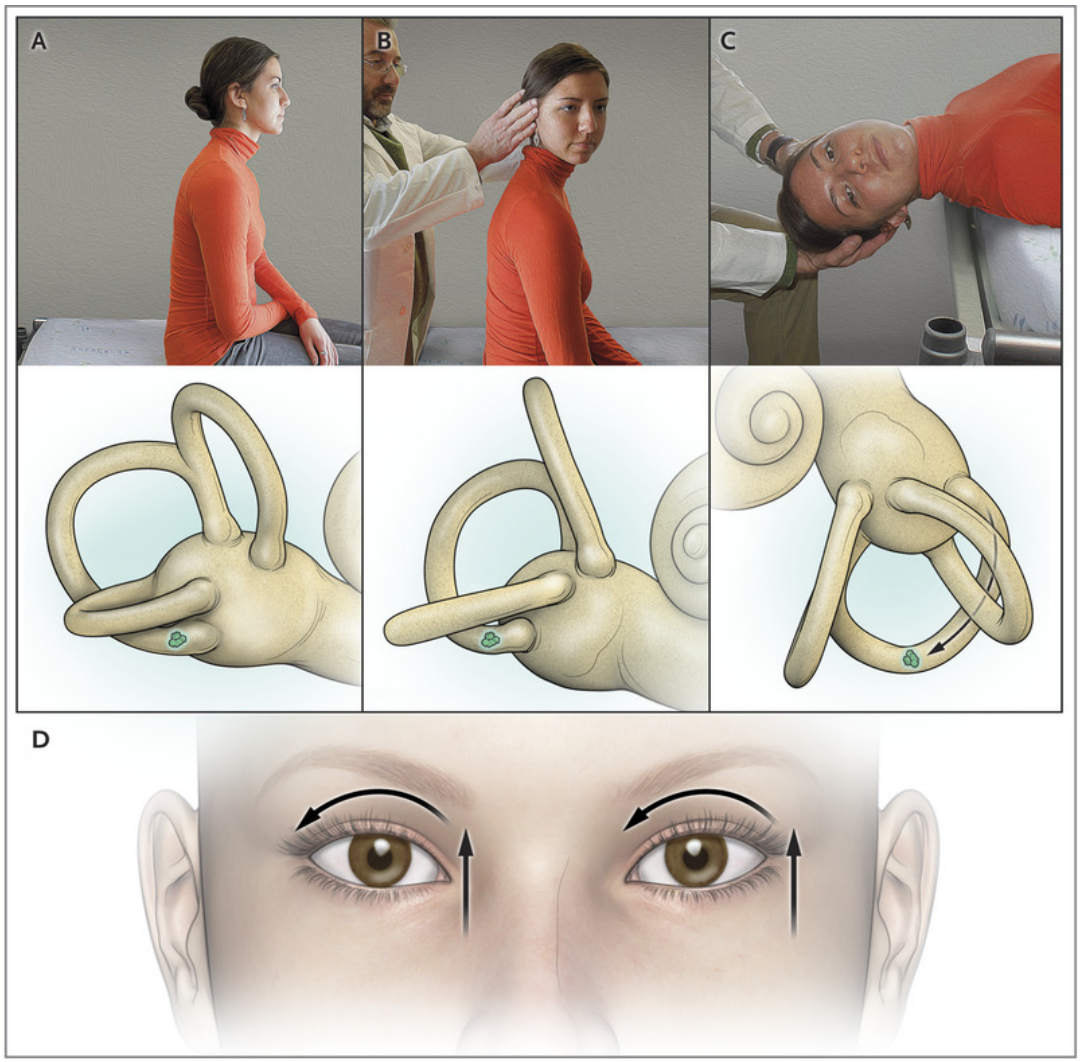

Figure 2.2: The Dix-Hallpike Maneuver Specialist orienting the patient into prescribed positions to move the otoconia within the semi-circular canal which generates nystagmus in the patient. Otoconia being guided out of the right posterioir semi-circular canal causes counterclockwise torsional- and upbeat- nystagmus as shown in D. Reproduced with permission from Kim and Zee, 2014, Copyright Massachusetts Medical Society.

2.1.4 Nystagmus

Vestibular nystagmus comprises of pattern of alternative slow eye drifts in one direction and rapid saccades in the opposite direction. The slow eye drifts are called slow phases and the rapid saccades are called quick phases. Intensity of nystagmus is measured by estimating the velocity of the slow phases. A patient with BPPV can thus be diagnosed by quantifying the intensity of the nystagmus they show during the Dix-Hallpike maneuver by measuring the Slow Phase Velocity (SPV).

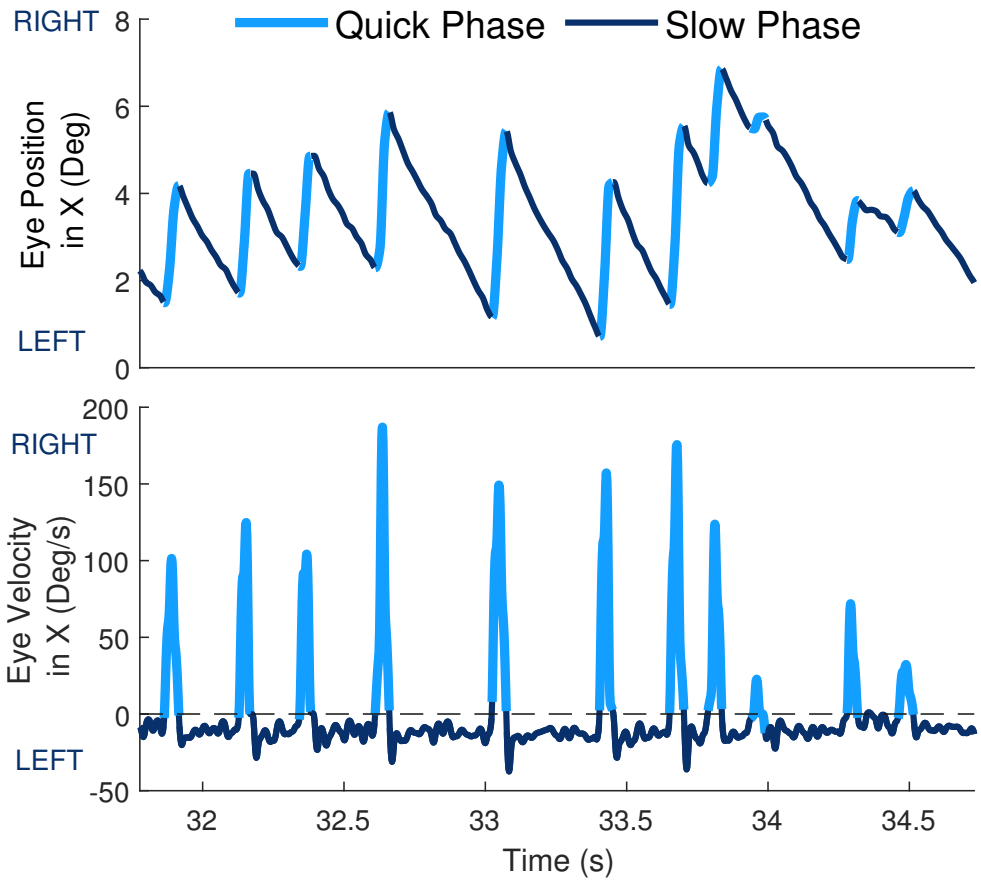

Figure 2.3: Nystagmus Trace A plot of horizontal eye position and velocity vs. time, obtained from a patient with nystagmus using the ICS Impulse Otosuite VOG goggles

2.1.5 Vestibular Function Tests

Vestibular Function Tests (VFTs) are used to assess the health of the vestibular system. They aid clinicians in identifying the cause of vertigo, dizziness, headache and other such symptoms in patients. They can also aid in the discernment between central disorders and vestibular dysfunctions. Different VFTs are used to assess different components of the vestibular system. General VFTs broadly consist of the following (as reviewed by Brandt and Strupp, 2005):

- Measurement of eye movements can reveal significant information regarding the vestibular functions. Eye movements are generally used to test canal (and pathways) functions. Two of the most commonly employed methods are Electronystagmography (ENG) in which eye position signals are recorded using electrodes and Video Oculography (VOG) in which eye position traces are obtained from image processing of eye videos. These are described further in Section 2.2. Video Head Impulse Test (vHIT) is another VFT in which eye movements are used to evaluate the vestibular system functioning. vHIT involves use of small, quick jerks of the head to assess the VOR.
- Measurement of otolith function using Vestibular Evoked Myogenic Potentials (VEMPs) involves the collection of Electromyography (EMG) signal evoked in response to acoustic stimuli. There are two different types of VEMPs - cervical (cVEMPS) and ocular (oVEMPS) - to test the functionality of the two otolith organs, saccule and utricle. cVEMPS is used to test saccule and inferior nerve and the EMG is recorded from

the sternocleidomastoid muscle. oVEMPs tests the utricle and superior nerve and the EMG is recorded from the extraocular muscles.

- Measurement of spatial perception using Subjective Visual Vertical (SVV) can help clinicians distinguish between peripheral and central vestibular or oculo-motor lesions. SVV involves an individual's ability to discern a vertical line relative to gravity in the absence of any visual cues and thus detects abnormalities in subject's tilt. The clinical SVV test is performed in a dark room within which subject has to align laser line to their perceived vertical. The SVV also tests utricle dysfunction and thus can also be used assessing otolith disorders.
- Measurement of posture using posturography enables clinical quantification of patient's posture and balance. Balance and postural stability depend on the functionalities the inner ear vestibular system and other senses like vision, somatosensory and proprioception. Thus, posturography can aid in postural research and can also reveal frequency of falls and side of lesion. Dynamic posturography estimates balance control in situations intended to isolate factors affecting balance by using a moving platform beneath the patient. Though this is not considered a VFT, many clinicians combine posturography with the other VFTs.

The present study focuses mainly on VOG based VFTs. Most commonly used VFTs that utilize VOG include the Dix Hallpike maneuver. This maneuver is used in the diagnosis of BPPV and it is classified as a positional test since the patient's body is moved from one position to another.

2.2 Eye Tracking

Eye movements have always been instrumental towards studying human behavior (Eckstein et al., 2017) as well as diagnosing various physiological conditions including Schizophrenia and attention deficit disorders (Harezlak and Kasprowski, 2018). Research in eye movements has been increasing vastly since the past decade not only for exploring nature of various diseases but also for probing applications in domains of human computer interaction and virtual reality. This can be attributed to advances in VOG technology: their portability, low-cost and ability to record reliable data have made them ubiquitous. Though other types of eye tracking methods exist, they've been vastly replaced by state-of-the-art VOG technology. These methods include:

- **Electro Oculography (EOG)**: Electrodes placed across subject's eyes record voltage differences generated during eye movements due to the dipole nature of eyeballs (voltage difference between cornea and retina). However facial/brain activity leads to significant noise and vertical eye movement recordings are unreliable (Brandt and Strupp, 2005).
- **Magnetic Scleral Search Coil**: Though this method offers accurate 3D eye movement recordings, it has limited clinical relevance due to its semi-invasive nature in which subjects must wear special contact lens that measures differences in magnetic flux during eye movements.
- **Scanning Laser Ophthalmoscope (SLO)**: Also called as fundus photography, this method was previously employed to obtain retinal images by scanning a laser across subject's eyes. However, this technique involves expensive setup and the subject's head must be fixed to a headrest.

2.3 Video Oculography

Video Oculography (VOG) is a video based method of tracking eye movements. VOG further includes infrared based benchtop system and infrared based wearable goggles (Holmqvist et al., 2011). Though there are other methods of tracking eye movements (scleral search coils and EOG), wearable VOG goggles would be the most suitable for the current purpose of clinical diagnosis stated in this paper due to its non-invasive nature and ease of use.

In the present study, patients in emergency departments of hospitals are to be diagnosed with BPPV. Hence, in order to facilitate accurate point-of-care diagnosis with minimal user training for data collection, eye tracking goggles are employed. One of the most common VOG goggles and software employed in clinics is the ICS Impulse Otosuite (GN Otometrics^{TM}, Taastrup, Denmark) system (Figure 2.4) (Bell et al., 2015; Roberts et al., 2016; Ross and Helminski, 2016; Otometrics, 2018).

Patients are fitted with the portable ICS Impulse goggles that are equipped with infrared cameras to image the eyes. Built-in calibration lasers are used to calibrate the goggles. The Otosuite software then detects the center of the pupil from which the eye traces are obtained and nystagmus is quantified.

Figure 2.4: VOG Goggles ICS Impulse Otosuite^{TM} video-occulography goggles used in the present study to record patient eye movements.

2.4 Otosuite Software

Data in the present study is collected using the ICS Impulse Otosuite^{TM} which is a combination of hardware and software specially devised for vestibular testing. The hardware includes a pair of lightweight goggles, used to acquire the eye movement data. The goggles are equipped with an infrared video camera and infrared Light Emitting Diodes (LED). The camera captures infrared light reflected off of the eyes to output real-time video feed of the eyes.

The software serves two purposes (Figure 2.5). It first extracts the center of the pupil from the video frames to display real-time eye movement trace. The software then uses the calculated eye movement trace (raw eye tracking signal) for nystagmus detection. The device is calibrated using laser targets projected forward from the goggles. These goggles are also equipped with a gyroscope and an accelerometer to measure head movements. For the present study, the raw eye tracking data and the head movement data are used to test proposed algorithm.

However, this system is found to have low specificity of **63%** for nystagmus detection (Chang et al., 2019). This can be attributed to several challenges including low sampling frequency of the goggles (60Hz) and presence of slow phases affecting computation. Moreover, bedside recordings from patients are susceptible to more noise and artifacts, than controlled laboratory conditions.

Hence, the present study aims to improve nystagmus detection to aid in making better diagnosis of dizzy patients. Towards this end, the proposed algorithm must be able to accurately estimate velocity of slow phases (which

quantify the intensity of nystagmus) after removing the intermediate quick phases. This entails robust detection of quick phases which are just rapid saccades, hence the next chapter explores different saccade (and other eye movement) detection algorithms published in the literature.

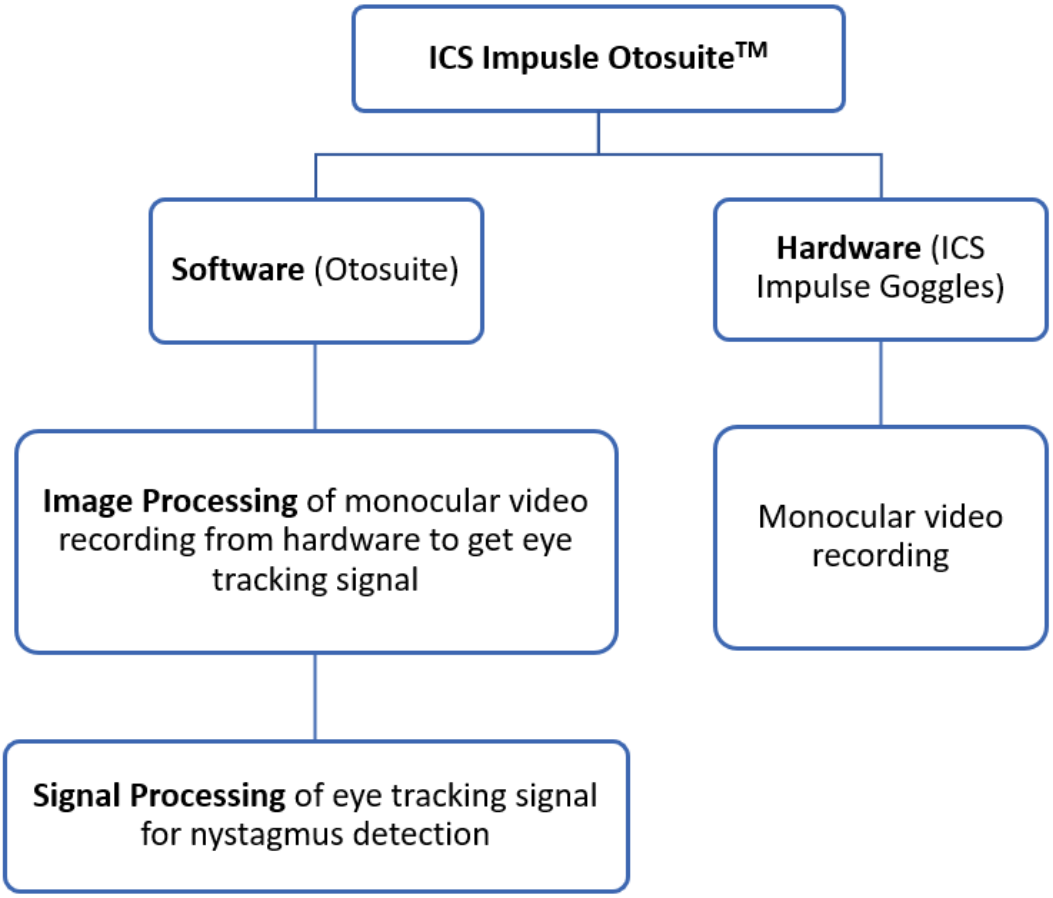

Figure 2.5: ICS Impuse Otosuite Sytem™ Components of the VOG system and their working

Chapter 3

Eye Movement Detection Methods

Eye movements can be broadly classified into six types: saccades, fixations, smooth pursuits, optokinetic reflexes, vestibulo-ocular reflex, and vergence (reviewed in Leigh and Zee, 2015). Most of the algorithms focus on identifying the first three movements, in both online and offline settings. Moreover, current state-of-the-art techniques to classify between different eye movements can be broadly classified into to four types: threshold, probabilistic, statistical and machine learning based algorithms as described below (Table 3.1).

As mentioned in the previous chapter, in order to estimate the intensity of nystagmus, velocity of slow phases (SPV) needs to be measured. This paper aims to first identify quick phases, remove them and then estimate the SPV from remaining slow phases. The quick phases in nystagmus are thought to be generated by similar mechanisms as that of saccades. Moreover, in the Dix-Hallpike maneuver used to diagnose BPPV, there is no stimulus and the patient being tested is under free viewing conditions in the dark. Patient can generate different eye movements that can affect the nystagmus detection. Hence, sections 3.1 and 3.2 describe an overview of the published

eye movement detection algorithms with special focus on saccade and smooth pursuit detection methods in free viewing experiments, that do not require stimulus as input.

Further, section 3.3 provides an overview of previous algorithms used for detection of nystagmus using eye tracking signals. The methods described in this section focus on the approaches employed, thus emphasizing on procedures for detecting nystagmus in general.

3.1 Saccade Detection Algorithms

Saccades are the quickest type of movements that humans can perform. These are rapid eye transitions from one point of fixation to another. Earliest comparison of different types of saccade detection algorithms can be traced back to the work done by Salvucci and Goldberg, 2000. They presented a comparison of Velocity Threshold (IVT), Dispersion Threshold (IDT), Hidden Markov Model (IHMM), Minimum Spanning Tree (IMST) and Area of Interest (IAOI) methods for the identification of fixations and saccades during an equation solving experiment involving students. IVT (eg., Barnes, 1981; Erkelens and Sloot, 1995) and IDT (Widdel, 1984) are threshold based algorithms which classify saccades and fixations using velocity and dispersion (spread between consecutive points) thresholds respectively.

IHMM (Salvucci and Goldberg, 2000) detects saccades by modeling eye movement distributions using a probabilistic approach, which makes it more robust than the threshold based methods. However, it is limited by the fact that the user needs to set 8 parameters without which its implementation would

be difficult. IMST (Goldberg and Schryver, 1995) is based on a graph and search tree algorithm which clusters the fixation points into one group. IAOI (Den Buurman, Roersema, and Gerrissen, 1981) classifies by thresholding the datapoints falling within a target region (area of interest) corresponding to the visual field. This paper concludes that IHMM and IDT achieve better results among the compared algorithms.

Komogortsev et al., 2010 also present a similar IHMM algorithm in addition to Identification by Kalman Filter (IKF) algorithm and compare these with IVT, IMST and IDT. The IKF models eye movements with position and velocity, outputting a predicted velocity that is compared with actual eye velocity using Chi-square test for classification between fixation and saccade. The IHMM method was shown to reveal higher accuracy of detection.

Nyström and Holmqvist, 2010 proposed an adaptive threshold based algorithm (NH) to distinguish between saccades and fixations. The threshold is adapted for each window of eye position signal based on the mean and standard deviation of the samples in that window. More recently, Friedman et al., 2018 modified the NH algorithm to include median velocity (to overcome the assumption that velocity samples have normal distribution as in the NH algorithm) and introduce different velocity thresholds. The paper presents the modified algorithm to perform better when also compared with the Identification by Random Forest (IRF) algorithm by Zemblys et al., 2018, where random forest is a machine learning based technique.

Hessels et al., 2017 proposed the Identification by Two-Means Clustering

(I2MC) algorithm, which uses unsupervised K-means clustering within windows of the eye velocity signal to obtain clustering weights that are used to separate between saccades and fixations. This paper also describes interpolation of missing data using Steffen's method (Steffen, 1990) which is shown to be more suitable for 1D signals than cubic spline as it reduces edge effects. Seven other algorithms were used for comparison: CDT (Veneri et al., 2011), BIT (Lans, Wedel, and Pieters, 2011), HC (Hooge and Camps, 2013), WSJ (Wass, Smith, and Johnson, 2013), IKF, IMST and NH. The last four were excluded from final analysis as they did not provide output for high noise data. Results indicated that I2MC performs better than the rest of algorithms when applied on data with high-noise.

Andersson et al., 2017 provide a detailed comparison of 10 different eye movement detection algorithms. Algorithms compared include IHMM,EK (Engbert and Mergenthaler, 2006), IKF, NH and LNS (Larsson, Nyström, and Stridh, 2013). Results conclude that LNS algorithm performs better than the other algorithms and NH is the runner up behind it. However, Pekkanen and Lappi, 2017 suggested a segmented linear regression approach for denoising and a Hidden Markov Model based method for classification, NSLR-HMM algorithm. When compared with the ten algorithms used in Andersson et al., 2017, the NSLR-HMM was shown to be more accurate than others in detecting saccades, fixations and smooth pursuits. Similarly, recently published REMoDNaV by (Dar, Wagner, and Hanke, 2019) resulted in higher accuracy than all the ten algorithms analyzed in Andersson et al., 2017.

Sheynikhovich et al., 2018 present an algorithm using the density based

clustering approach (Rodriguez and Laio, 2014) by computing correlation of feature vectors of selected peaks to detect microsaccades. And prior to that, Otero-Millan et al., 2014 proposed a K-means clustering approach, OM. The density based clustering approach was shown to obtain better results when compared against OM and EK. However, this algorithm relies on the assumption that noise events must be sufficiently different from a typical microsaccade and for reliable detection, the dataset needs to have sufficient number of microsaccades to form a cluster. When trying to compare the density based approach to the IPF algorithm (Daye and Optican, 2014), which is based on bayesian modeling, Sheynikhovich et al., 2018 have indicated that "*the choice of IPF's parameters on a per-subject basis is a problem that makes practical application of this method and its comparison with other algorithms difficult*". Comparison with BMD (Mihali, Opheusden, and Ma, 2017), a bayesian algorithm which provides inference through statistical modeling of eye position via posterior distribution of events, was stated to be not possible due to different settings used during eye movement recording.

Though statistical methods like CDT and Mulligan, 2018 use thresholds for differentiating between fixations and saccades, the data is subjected to statistical test in order to apply these thresholds. CDT analyse variance and covariance while Mulligan, 2018 perform t-test within windows while Veneri et al., 2010 utilize the F-test. Korda et al., 2018 use the largest lyapunov exponent statsitic and similarly Mould et al., 2012 utilize the gap-statistic.

Recent developments in Machine Learning has seen a surge in its application on eye tracking data. Zemblys, 2017 provide an overview of different

machine learning techniques applied on VOG data. Hoppe and Bulling, 2016 provide one of the initial methods using CNNs for eye movement classification, with a resulting accuracy of 75%. Bellet et al., 2018 also proposed a U-Net (NN used for image segmentation) inspired CNN, called U'n'Eye, for saccade detection. Startsev, Agtzidis, and Dorr, 2019 presented a CNN-BLSTM based method for detection of all three types of eyemovements. Recently, Zemblys, Niehorster, and Holmqvist, 2019 developed gazeNet, by using a Recurrent Neural Network (RNN) combined with CNN. However, comparison between the different types of deep learning methods presented needs to yet be studied.

3.2 Smooth Pursuit Detection Algorithms

Smooth pursuit movements allow us to track moving objects over a period, following different trajectories. Komogortsev and Karpov, 2013 proposed three threshold based algorithms to identify smooth pursuit in addition to fixations and saccades. These are: Modified version of IVT Algorithm (IVVT), Identification by Velocity and Movement Pattern (IVMP) and Identification by Velocity and Dispersion Threshold (IVDT). Results concluded that IVDT surpasses the performance of the other two, and that its performance is less influenced by thresholds. They also introduced ideal behavior scores which are used in automatic selection of optimal thresholds with an objective function. However, this method requires annotated data or at least known stimulus presentation. Larsson et al., 2016 compared IVDT with their multi-modal event detection algorithm for unconstrained head movements and results concluded that their algorithm performs better. However, their proposed

algorithm is also dependent on stimulus trajectory. Similarly, Larsson et al., 2015 propose a method for high speed eye trackers that was shown to perform better than the IVDT.

Within the probabilistic methods, recent developments include the Identification by Bayesian Decision Theory (IBDT) by Toivanen, Pettersson, and Lukander, 2015 that is presented to identify smooth pursuit in addition to saccades and fixations. In this method, the fixation and saccadic likelihoods are initialized based on the eye data and are modeled as Gaussian distributions. When compared to the IVDT algorithm by Komogortsev and Karpov, 2013, the IBDT was shown to achieve better detection.

Recently proposed MBSDC method by (Wadehn et al., 2019) is based on a mechanistic model of the eye from the kinematic and neural signals of saccade, fixation and smooth pursuit. This method was shown to perform similar to the IRF. However, this method is only applicable to horizontal eye position and requires higher computational cost due to Kalman filtering involved in the intermediate steps of linear state space modeling of the eye. Additionally, REMoDNaV, an adaptive threshold based technique, also detected smooth pursuits in addition to fixations, saccades and PSOs and was shown to perform better than the ten algorithms in Andersson et al., 2017.

Startsev, Agtzidis, and Dorr, 2019 proposed a deep learning method using CNN-BLSTM to detect smooth pursuit in addition to fixations and saccades. Though this method achieves higher accuracy for smooth pursuit, it still has 34% error rate on the tested data while the LNS was found to perform better in case of saccades among the comparisons.

3.3 Nystagmus Detection Algorithms

Allum, Tole, and Weiss, 1975, Baloh, Kumley, and Honrubia, 1976, Ranacher, 1977 and Barnes, 1981 are some of the initial works done on analysis of nystagmus, most of which required a human operator. These algorithms were tailored for nystagmus during VOR and OKN stimulation. Rey and Galiana, 1991 presented a method based on autoregressive modeling but it takes in head position as input for the analysis. Similarly, Arzi and Magnin, 1989 described a fuzzy set approach towards the analysis of nystagmus in VOR and OKN that is automatic but requires stimulus trajectory.

Juhola, 1988 proposed a nystagmus detection algorithm by using a recursive digital filter. It was shown to function reliably only for slow phase velocity above $5^o/s$ while filter adaptation was susceptible to artifacts and noise. Engelken and Stevens, 1989 describe a method based on non-linear filters of Order Statistics, specifically by using adaptive asymmetrically trimmed mean-filter that is independent of stimulus projection. This method was based on the assumption that the eyes spend more time in slow phase than in quick phase within a window. Juhola, Aalto, and Hirvonen, 2007 used NN in their method but it is dependent on stimulus trajectory. Similarly, Ranjbaran, Smith, and Galiana, 2016 use the head position data to model the VOR system and propose an iterative method that is initialized using K-means.

Roberti, Russo, and Segrè, 1987, Reccia, Roberti, and Russo, 1989, Reccia, Roberti, and Russo, 1990, Miura et al., 2003, Hosokawa et al., 2004 and Abel, Wang, and Dell'Osso, 2008 are some works that utilize frequency domain analyses including Wavelet and Fourier transforms. Spectral analysis for

nystagmus has not been shown to be reliable as the frequency of quick phases can highly overlap with that of the noise present in the signal and is most often based on the assumption that the beats have similar structure.

Pander et al., 2012 proposed a method on ENG signals which are first pre-processed using myriad, IIR, and FIR filters after which a nonlinear detection function is computed from the filtered ENG signal. Peaks in the detection function correspond to quick phases which are detected by adjusting a threshold using fuzzy clustering. The parameters in this algorithm are voltage dependent and their conversion to degrees for VOG data might be challenging.

3.4 Summary

As described above, eye movement detection algorithms can be broadly classified into to four types: threshold, probabilistic, statistical and machine learning based algorithms as shown in Table 3.1. These algorithms were proposed to detect eye movements such as saccades, fixations and/ or smooth pursuit. Table 3.2 shows published works that compare performance of various state-of-the-art eye movement detection algorithms.

As can be seen, there exists vast range of algorithms implemented using simple techniques to advanced methods for detection of saccades, fixations and smooth pursuit. Though advanced techniques might offer better results, they would need user training in order to set the algorithm parameters that can achieve the best results. Since eye movements are used by many researchers not familiar with such advanced concepts, methods based on signal processing concepts and simplistic approaches could provide a solution. However, they

must be developed rigorously for accurate detection of eye movements.

Moreover, most of prior methods for nystagmus detection, as seen in section 3.3, relied on the input of a stimulus or a head movement signal. However, in contrast to the case for normal subjects, the jerk nystagmus in BPPV patients occurs in the absence of vestibular or optokinteic stimulus. Additionally, as will be described in the next chapter, bedside recordings from patients in the emergency department are susceptible to more noise and artifacts than under controlled laboratory conditions. This further necessitates the proposed algorithm to be robust to noise and artifacts.

Type	Algorithm
Threshold-based	• IVT (eg., (Barnes, 1981)) • IAOI Den Buurman, Roersema, and Gerrissen, 1981 • IDT (Widdel, 1984) • Behrens and Weiss, 1992 • EK (Engbert and Mergenthaler, 2006) • Berg et al., 2009 • Dorr et al., 2010 • IMSF (Behrens, MacKeben, and Schröder-Preikschat, 2010) • NH (Nyström and Holmqvist, 2010) • BIT (Lans, Wedel, and Pieters, 2011) • HC (Hooge and Camps, 2013) • WSJ (Wass, Smith, and Johnson, 2013) • IVVT (Komogortsev and Karpov, 2013) • IVMP (Komogortsev and Karpov, 2013) • IVDT (Komogortsev and Karpov, 2013) • LNS (Larsson, Nyström, and Stridh, 2013) • Stuart et al., 2014 • LNS15 (Larsson et al., 2015) & LNS16 (Larsson et al., 2016) • NSLR-HMM (Pekkanen and Lappi, 2017) • Modified NH (Friedman et al., 2018) • REMoDNaV (Dar, Wagner, and Hanke, 2019)

Probablistic/ Bayesian	• Using autoregressive model & Kalman filter (Sauter et al., 1991) • IHMM (Salvucci and Goldberg, 2000) • Using Kalman filter Kumar et al., 2008 • IKF (Komogortsev et al., 2010) • Tafaj et al., 2012 • Liston, Krukowski, and Stone, 2013 • IPF (Daye and Optican, 2014) • BMM (Kasneci et al., 2015) • EM-GMM (Toivanen, Pettersson, and Lukander, 2015) • IBDT (Santini et al., 2015) • Using advanced Kalman filter (Toivanen, 2016) • BMD (Mihali, Opheusden, and Ma, 2017) • MBSDC (Wadehn et al., 2019)
Statistical	• Using F-test (Veneri et al., 2010) • CDT (Veneri et al., 2011) • Using gap-statistics (Mould et al., 2012) • Using lyapunov exponent (Korda et al., 2018) • Using t-Test (Mulligan, 2018)
Machine Learning - Based	• IMST (Goldberg and Schryver, 1995) • IHMM (Komogortsev et al., 2010) • Shape features (Vidal, Bulling, and Gellersen, 2012) • Vidal et al., 2013 • K-means clustering, OM (Otero-Millan et al., 2014) • Using SVM & CNN (Anantrasirichai, Gilchrist, and Bull, 2016) • Using CNN (Hoppe and Bulling, 2016) • I2MC (Hessels et al., 2017) • IRF (Zemblys et al., 2018) • Density based clustering (Sheynikhovich et al., 2018) • U'n'Eye (Bellet et al., 2018) • Using CNN-BLSTM (Startsev, Agtzidis, and Dorr, 2019) • gazeNet (Zemblys, Niehorster, and Holmqvist, 2019)

Table 3.1: Classification of Algorithms Eye movement detection algorithms classified based on their approach

Publication	Algorithms Compared	Result
Salvucci and Goldberg, 2000	IHMM, IVT, IDT, IMST, IAOI	IHMM
Komogortsev et al., 2010	IHMM, IKF, IVT, IDT, IMST	IHMM
Komogortsev and Karpov, 2013	IVVT, IVDT, IVMP	IVDT
Larsson et al., 2015	LNS15, IVDT	LNS15
Santini et al., 2015	IBDT, IVDT	IBDT
Larsson et al., 2016	LNS16, IVDT	LNS16
Mihali, Opheusden, and Ma, 2017	BMD, OM, EK	BMD
Hessels et al., 2017	I2MC, CDT, BIT, HC, WSJ, IKF, IMST, NH	I2MC
Andersson et al., 2017	LNS, NH, IHMM, IKF, CDT, BIT, IVT, IDT, IMST, EK	LNS
Pekkanen and Lappi, 2017	NSLR-HMM, LNS, NH, IHMM, IKF, CDT, BIT, IVT, IDT, IMST, EK	NSLR-HMM
Friedman et al., 2018	Modified NH (MNH), NH, IRF	MNH
Sheynikhovich et al., 2018	Density based clustering (clustDb), OM, EK	clustDb
Wadehn et al., 2019	MBSDC, IRF	IRF
Dar, Wagner, and Hanke, 2019	REMoDNaV, LNS, NH, IHMM, IKF, CDT, BIT, IVT, IDT, IMST, EK	REMoDNaV
Startsev, Agtzidis, and Dorr, 2019	CNN-BLSTM, Dorr et al., 2010, Berg et al., 2009, LNS15, IVMP, IVDT, IVVT, IKF, IHMM, IVT, IMST, IDT	CNN-BLSTM (for smooth pursuit)

Table 3.2: Comparison of Algorithms Papers that compare different proposed algorithms

Chapter 4

Data

4.1 Data Resource

Data used in the current study was obtained from an ongoing multi-center clinical trial, **AVERT** (Acute Video-oculography for Vertigo in Emergency Rooms for Rapid Triage) (Newman-Toker, 2014), that compares diagnostic accuracy and actual clinical outcome between eye movement (VOG) based diagnosis and standard diagnosis in patients with dizziness and vertigo. Patients presenting with a chief complaint of acute vertigo or vertigo were included upon their consent. Patients with critical illness, level-one trauma, unstable cardiac status, under the age of 18 years old, cranial-cervical trauma, altered mental status, or pregnancy were excluded.

Data was collected using a portable Video Oculography (VOG) device, ICS Impulse, with Otosuite software (GN Otometrics^{TM}, Taastrup, Denmark) at a rate of 60Hz. Eye position was calibrated in the device using laser targets projected from the goggles to the front. Patients were then subjected to a battery of VOG tests, including Dix-Hallpike positional test, as listed below:

1. Latero-pulsion test
2. Gaze tests with fixation: center, downward, leftward, rightward, and upward gaze
3. Skew deviation test in sitting position
4. Lateral-canal vHIT test
5. Gaze tests without fixation: center, leftward and rightward gaze
6. Head shaking test with vision denied for head-shaking nystagmus
7. Positional tests with vision denied: left Dix-Hallpike test, right Dix-Hallpike test, left roll test, right roll test
8. Bow-Lean tests: chin-to-chest test and head-extended backwards
9. Skew deviation test in supine position

4.2 Data Extraction

The data of each patient tested was downloaded from the database. This included the raw eye movement and head movement data, stored in a Comma Separated Values (CSV) file and the slow phase velocities computed by the Otosuite software stored in an eXtensible Markup Language (XML) file. There is a single CSV file for each patient that includes the raw eye position and head position data for all VFTs performed. The XML files store data in the form of nodes which can have subnodes to store structured data. XML files are useful for efficiently storing data having large number of groups or classes. Otosuite^{TM} stores the SPV and other related results for all VFTs using this format. MATLAB has robust in-built functions to read XML files using the ***xmlread*** command. Further code was written to extract the eye position

data and the final output of software from each of the categorized nodes (corresponding to the different tests) from the XML files. Extracted data comprises of:

1. Patient ID
2. Type of test and Test ID
3. Average frame rate
4. Start date and time
5. End date and time
6. Vision denied indicator
7. Raw eye position data for each test (degrees)
    - Horizontal (X)
    - Vertical (Y)
    - Torsional (T)
8. Raw eye position data for each test (pixels)
    - Horizontal (X)
    - Vertical (Y)
9. Raw head position data in Quaternions for each test (Q_1, Q_2, Q_3, Q_4)
10. Otosuite^{TM} Results (for X, Y and T components) (in Deg/s):
    - Slow Phase Velocities
    - Peak Slow Phase Velocity (SPV)
    - Average SPV
    - Maximum SPV
    - Minimum SPV
    - Peak SPV Time (in ms)

4.2.1 Head position data

Head position is described using quaternions in the Otosuite^{TM} system. Quaternions are a number system beyond the complex number system and they can be written as follows:

$$Q = Q_1 + Q_2 i + Q_3 j + Q_4 k$$

where Q_1, Q_2, Q_3, and Q_4 are real numbers and i, j and k represent unit-vectors along an orthogonal 3D basis (Finkelstein et al., 1962). They are most commonly used to represent rotations of objects in the 3D world. In this case head rotation and velocity can be obtained from the raw quaternion data provided by the Otosuite^{TM} software.

4.2.2 Torsional data

Apart from horizontal and vertical eye movements, human eyes can also move in a third component. This is the rotation of eyes about the axis of line of sight. Such type of rotational eye movements are categorized as **torsional** eye movements. Horizontal and vertical eye position data is calculated by obtaining pupil center from the VOG data. However, pupil center does not provide torsional information and hence calculating torsional data relies on other strategies. Obtaining accurate torsional data from VOG is still an active area of research (Otero-Millan et al., 2015). The torsional data captured by Otosuite^{TM} software is shown to be unreliable and hence the torsional component is excluded from any further computations. Only horizontal (X) and vertical (Y) components are considered for the proposed algorithm.

4.3 Manual Labeling

For the present study, data from **103 patients** was extracted. These patients were subjected to the Dix-Hallpike left and Dix-Hallpike right tests along with the other 8 tests listed in section 4.1. However, not all tests were done in all patients due to various reasons. In total 1054 test recordings were extracted from the data of these 103 patients which included **157 recordings** of the Dix-Hallpike tests.

For each of the Dix-Hallpike tests, both horizontal and vertical recordings were considered. A neurology expert manually visualized all the recordings and labelled whether nystagmus was present/ absent. Further, the expert also recorded output from the Otosuite^{TM} software. Thus, for each of the tests conducted on each of the patients, manual result and Otosuite^{TM} software result were noted in a CSV file. This was used in comparing final results from proposed custom algorithm and Otosuite^{TM} software.

4.4 Challenges with Data

As iterated before, due to the bedside nature of the data collection process the eye tracking data from VOG goggles in the present study are susceptible to more noise and artifacts than under controlled laboratory conditions. Apart from blinks (or periods when the eyes are closed), there are other artifacts present in eye tracking data. Below are some of the challenges that need to be addressed for an accurate detection of nystagmus from the eye data.

4.4.1 Missing Data

Eye tracking software can sometimes skip recording video frames and this could be due to delayed computation by the computer (Figure 4.1). Such missed frames are often interpolated if they are shorter than a threshold duration.

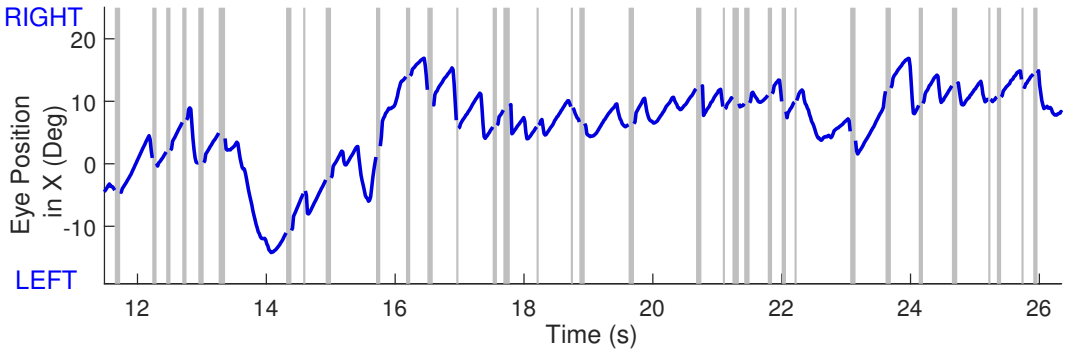

Figure 4.1: Missing data Shaded grey regions represent periods of missing data

4.4.2 Loss of Pupil Center

Sometimes, eye lashes of patients can interfere with the pupil center detection leading to artifacts in the eye trace. These artifacts most often appear as high frequency but low amplitude spikes in signal (Figure 4.2) and can often interfere with saccade detection as they can closely resemble saccades.

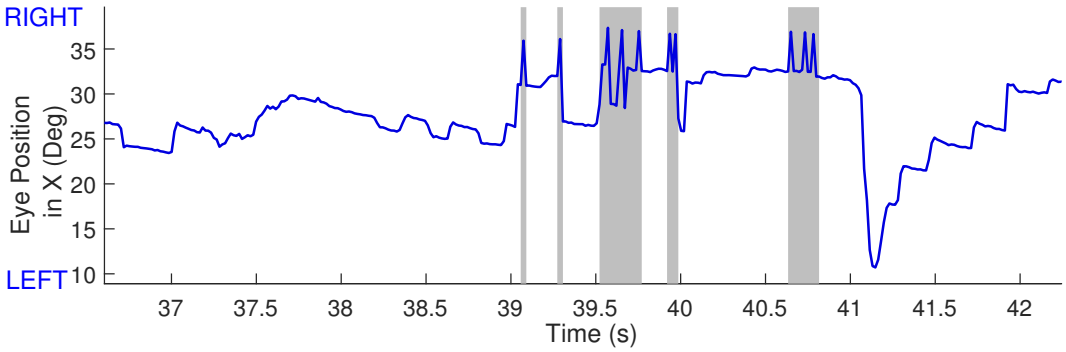

Figure 4.2: Spiky data Shaded grey regions represent periods of loss of pupil center

4.4.3 Patient Drowsiness

When patient is drowsy, their eye movements follow smooth trajectories as in Figure 4.3. Since these are low frequency (longer duration than saccades) and high velocity periods, they're not detected as quick phases.

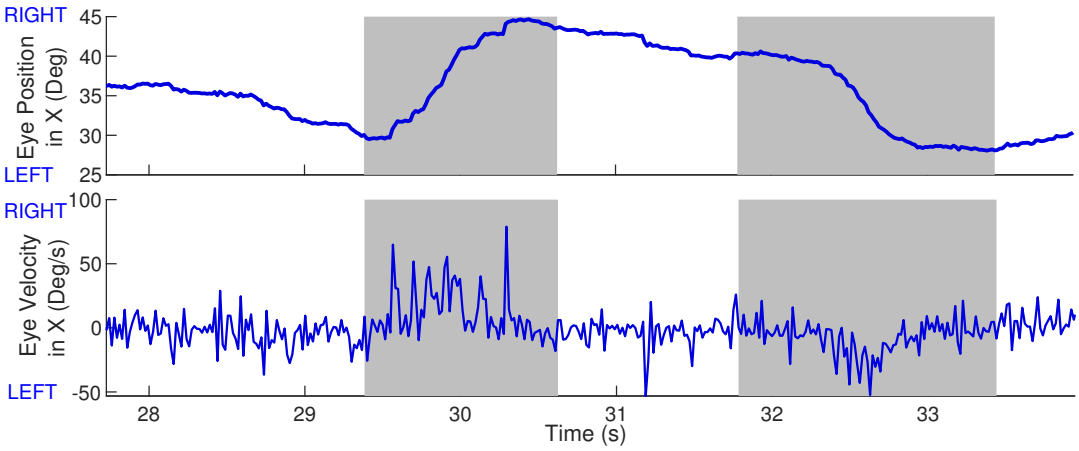

Figure 4.3: Patient Drowsiness Example of eye position signal during drowsy state

4.4.4 Noise

In some cases, eye position data has high noise and it is not possible to identify any kind of eye movement (Figure 4.4). This may be due to poor illumination, bad threshold for pupil detection or a pupil that is too small or too large.

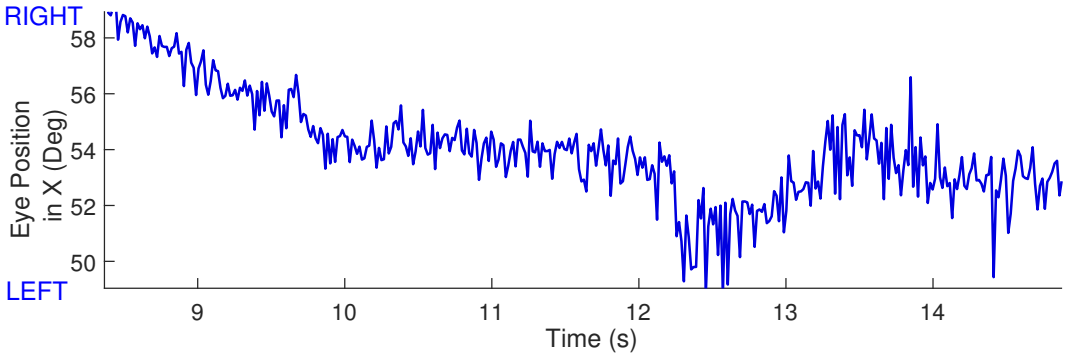

Figure 4.4: Noisy data Example of eye position signal corrupted with noise

4.4.5 Presence of Slow Phase

Nystagmus is a cyclic eye movement condition composed of alternative quick phases and slow phases. Quick phases are in the opposite direction to slow phases. The intermediate slow phases occur with a certain velocity that forms a non-zero baseline as shown in Figure 4.5. Detection of quick phases in the presence of such a baseline slow phase velocity (SPV) becomes challenging.

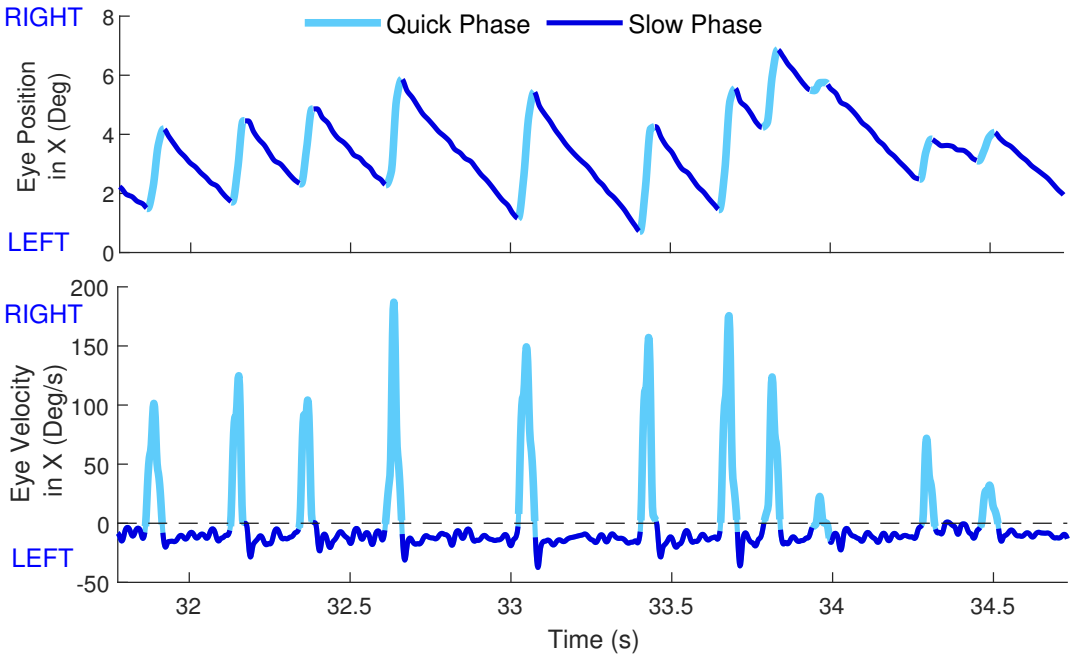

Figure 4.5: Presence of slow phase Example eye position signal from patient with nystagmus. Slow phase velocity can be seen as a non-zero baseline.

Chapter 5

Methodology

The present algorithm consists of four stages: pre-processing (section 5.1), peak detection and selection (section 5.2), clustering (section 5.3), and final SPV estimation (section 5.4). Figure 5.1 provides an overview of the steps involved in each of the four stages of the proposed custom algorithm. Due to the modular nature of the proposed algorithm, each stage can be improved independently; changing one stage would not affect any of the subsequent stages.

Most previous studies combined horizontal (X) and vertical (Y) components for saccade detection. However, in the present study computation was done on the two components separately. This was chosen since nystagmus can be present in either horizontal component or vertical component or simultaneously in both the components. Hence, the X and Y eye velocities were calculated separately for the present algorithm. Moreover, all the steps described in the following pages are performed separately on each component (without combining X and Y components of eye data) except for in the pre-processing stage.

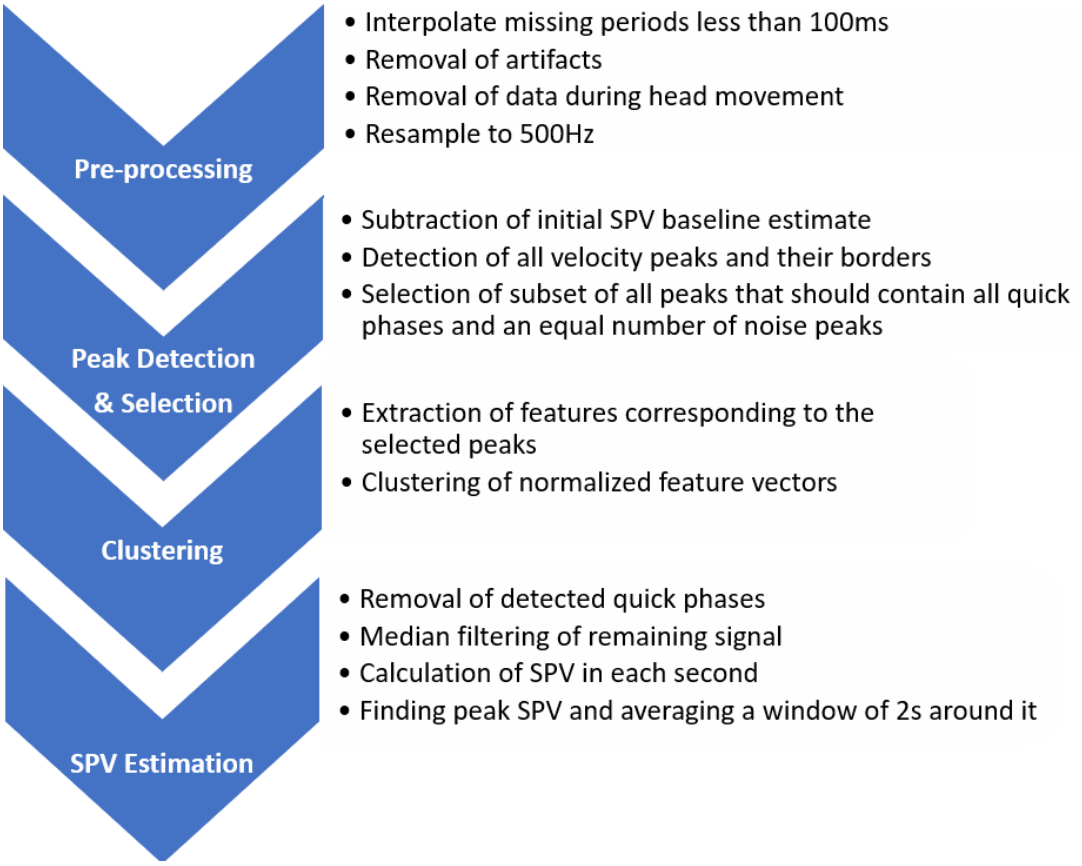

Figure 5.1: Functional Overview of Algorithm Description of steps involved in each stage of custom algorithm

The raw eye tracking data is first preprocessed to remove noise and corruptive artifacts that are higher in bedside recordings compared to controlled laboratory conditions. In order to detect nystagmus, proposed method first identifies the quick phases, which are then removed to obtain slow phases from which the SPV is computed that quantifies the intensity of the nystagmus. Since are generated by similar mechanisms as that of saccades, this method can also be used for saccade detection. Moreover, use of the algorithm does not require user training.

Proposed method employs a two-pass system for saccade detection, in

comparison to the traditional algorithms. From the eye movement recording, overall velocity peaks are detected and subsequently a subset of them are selected based on a computed threshold. This selection of peaks is based on rate factor which is computed from the physiological observation that rate of saccades is limited to 1-6 per second. The peak selection ensures that data points are balanced and possess the capacity to form clusters, thus aiding in the subsequent clustering stage. As can be seen, this is a novel top-down approach that is robust and easy to implement.

Proposed method incorporated clustering since it is an unsupervised method and has the promise of robust classification. Clustering techniques do not require training with data (and consequently eliminating the laborious and time-consuming process of manual labeling) while also being independent of the type of eye tracker used for data collection. Most importantly, clustering does not require user training. In the present study, Spectral Clustering was chosen for classifying the selected peaks.

5.1 Pre-processing

Eye movement data must be pre-processed before further analysis. The pre-processing stage aims to remove artifacts and noise in the data. One of the artifacts, eye blinks, are already processed by Otosuite^{TM} to output flat periods. Steps described below are performed to address the challenges listed in section 4.4. For the pre-processing stage, both X and Y components are considered together since artifacts in one component can affect eye movement recording in the other component. The samples in these periods identified as bad data

are removed (labelled as missing data) from the final processed signals.

5.1.1 Interpolation of dropped samples

In order to maximize the amount of eye movement recording available for nystagmus detection, imputation of dropped frames is performed using interpolation. Periods of dropped data shorter than 100ms (6 samples at 60Hz) are interpolated using Steffen's method (Steffen, 1990). This method was chosen and adapted previously by Hessels et al., 2017 and is shown to be better than cubic spline interpolation as it decreases edge effects.

5.1.2 Removal of out of range eye position/ velocity/ jerk data

Eye position data might also include some abrupt changes that would not be possible physiologically. These abrupt changes happen due to errors in pupil tracking and are found more clearly in derivatives of the position signal. In the present study, velocity and jerk are used. They are defined as below:

$$\text{Velocity} \Rightarrow \qquad v_x = \frac{dx}{dt} \qquad v_y = \frac{dy}{dt}$$

$$\text{Acceleration} \Rightarrow \qquad a_x = \frac{dv_x}{dt} \qquad a_y = \frac{dv_y}{dt}$$

$$\text{Jerk} \Rightarrow \qquad j_x = \frac{da_x}{dt} \qquad j_y = \frac{da_y}{dt} \qquad J = \sqrt{j_x^2 + j_y^2}$$

where,

x = horizontal component of the eye position

y = vertical component of the eye position

t = time in seconds

First, samples with v_x or v_y greater than $1000^o/s$ are found. However it is not sufficient to remove just the samples above this threshold, but also the entire period of such abrupt changes: beginning from the initial starting point to the ending point where these abrupt change peaks subside. Thus, each of these out of range velocity peaks is removed iteratively by finding its beginning and end points. Next, similarly samples with jerk, J, greater than $5 \times 10^{6^o}/s^3$ are found. Beginning and ending points of each of these out of range jerk samples are found and removed.

5.1.3 Removal of high fluctuation noise/ software artifacts

As described in section 4.4, sometimes the VOG software can compute incorrect pupil center or continuously switch between two possible pupil centers. This could be attributed to factors such as interfering eye lashes, software computational error, environmental disturbances etc. These periods of loss of pupil center can be detected by using the fact that human eye cannot make more than 15 saccades in a second (Lee, Badler, and Badler, 2002; Møller et al., 2002).

In the present method, the signal is windowed into periods of 200ms and the number of eye movement transitions are computed within each of these windows. Windows that exceed the physiological limit (for 200ms, the eye can make no more than 3 saccades) contains this type of high fluctuation noise and are removed accordingly. Eye position data between 34s and 38s in Figure 5.2b shows an example of periods when pupil center is lost and the resulting processed signal after removing them.

5.1.4 Removal of data during head movement

Positioning of patient during the Dix-Hallpike test would result in movement of their head. The eye data collected during head movements must be detected and removed as head movements would elicit a normal VOR response that could be interpreted as nystagmus if not removed. in the present study, head velocity is calculated using quaternion math from the raw head co-ordinates output by the software that are recorded using an embedded gyroscope on the VOG goggles. Eye tracking data is removed during head movements greater than $10^{o}/s$ and within a window of 400ms before and after such periods.

5.1.5 Removal of periods of good data between bad data

Periods of good data, less than 160ms in duration , in between bad data are also probably bad data. Hence samples in these periods are removed by using the closing (morphological) filter. In the image processing domain, this filter is used to remove small holes in the image. Translated to the one dimensional signal processing domain, it can be used to remove the small periods of samples in between missing data (the samples removed due to being identified as bad data). Using a window of 10 samples i.e., presence of 10 or less good samples in between periods of detected bad data are thus removed and labelled as missing data.

5.1.6 Resampling to 500Hz

The cleaned eye position data is then upsampled to 500Hz, taking care that missing samples do not propagate during the upsampling.

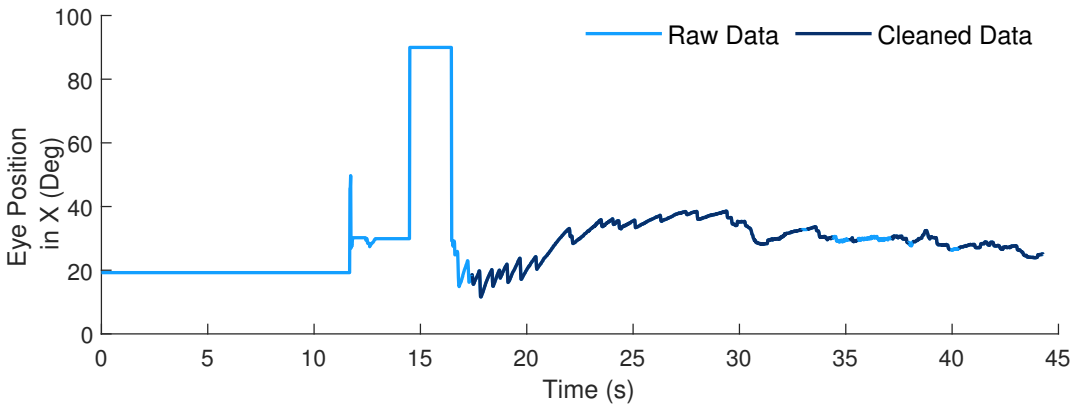

(a) Example of a pre-processed eye position signal

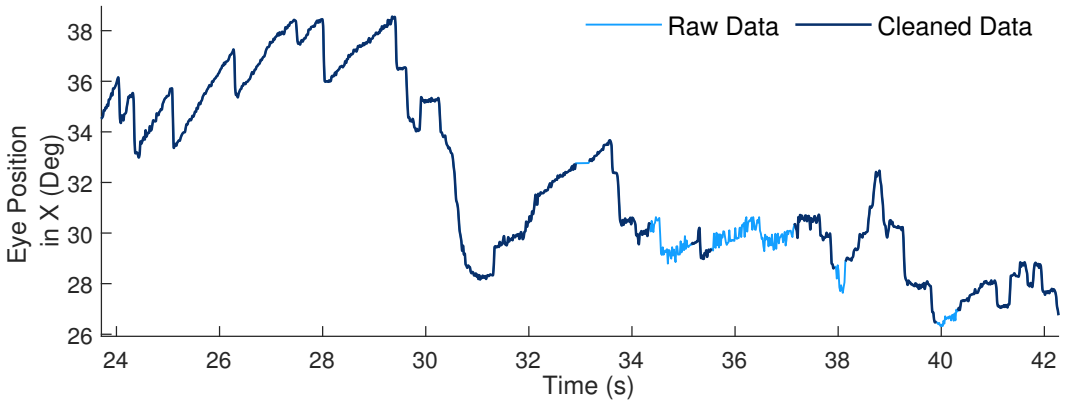

(b) Removal of periods with loss of pupil center

Figure 5.2: 5.2a shows example of pre-processed eye position signal in X component from a patient with nystagmus. 5.2b shows a zoomed in version of the signal in 5.2a showing periods of high fluctuation noise

Figure 5.2 showing horizontal eye position signal obtained from a patient with nystagmus (recorded using the ICS Impulse Otosuite^{TM} system) will be used as example for subsequent steps throughout this chapter.

5.2 Peak Detection and Selection

5.2.1 Peak Detection

(a) ***Subtraction of initial SPV baseline estimate***

In order to find velocity peaks and their end points, the eye velocity of individual components is smoothed over a window of 5 samples (Engbert and Kliegl, 2003) to suppress noise. Smoothed eye velocity was obtained for each component separately as below:

$$v_i = \frac{F_s}{6}(p_{i+2} + p_{i+1} - p_{i-1} - p_{i-2})$$

where,

F_s = sampling frequency (500Hz)

p_i = eye position (either horizontal or vertical component) at time i

v_i = instantaneous velocity at time i

An initial SPV baseline estimate is then found by iteratively excluding the highest 5% velocities in a running window of 1s and median filtering the remaining velocity values within the window. This results in an initial low pass velocity which is the initial SPV baseline estimate (Figure 5.4). This low pass velocity estimate is then subtracted from the eye velocity to give an approximate zero baseline velocity.

(b) ***Detection of all velocity peaks and their borders***

Humans have a physiological limit of at least 30ms time gap between consecutive saccades (Møller et al., 2002). Hence, all velocity peaks that are separated by at least 30ms (minimum intersaccadic interval) are

detected in the velocity obtained from the previous step (Figure 5.5). The corresponding start and end points of each peak are accordingly found.

5.2.2 Peak Selection

From the detected peaks, median absolute deviation of the prominence (height of peak velocity from the baseline rather than from zero) of all the peaks is found. This is multiplied by lambda (λ) (Engbert and Kliegl, 2003) to get prominence threshold. All the peaks with prominence above this threshold are counted. This corresponds to approximate rate of saccades, R_1. Multiplying this R_1 with a rate factor, F, would give rate, R_2 which should include all the saccades or QPs and an almost equal number of noise peaks (Figure 5.3). Selected peaks are shown in Figure 5.6.

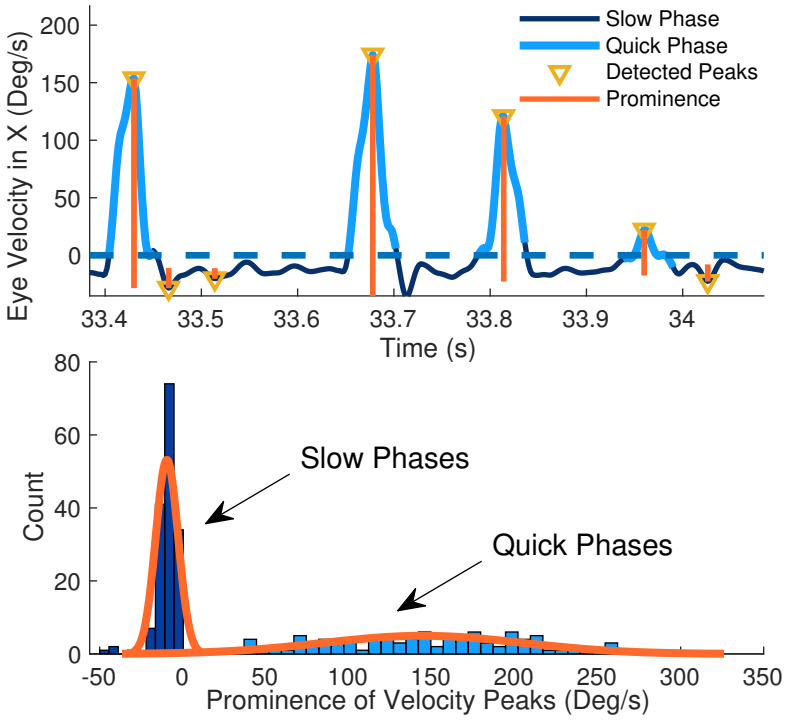

Figure 5.3: Prominence distribution Rate of saccades obtained from prominence

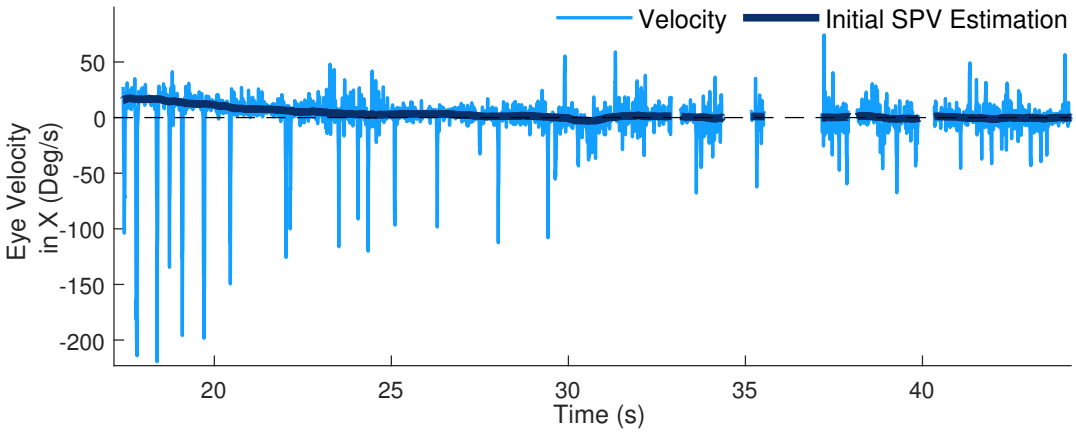

Figure 5.4: Initial SPV baseline estimate subtracted for period detection

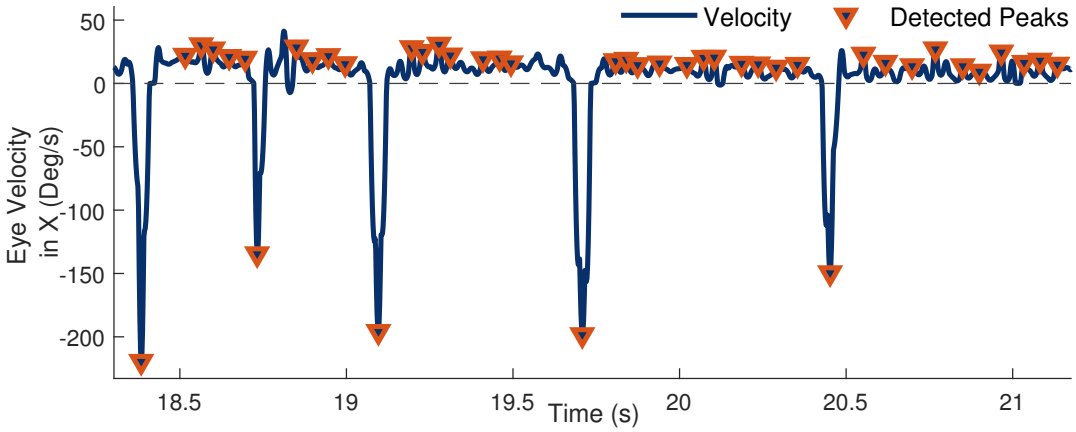

Figure 5.5: Peak detection All detected velocity peaks

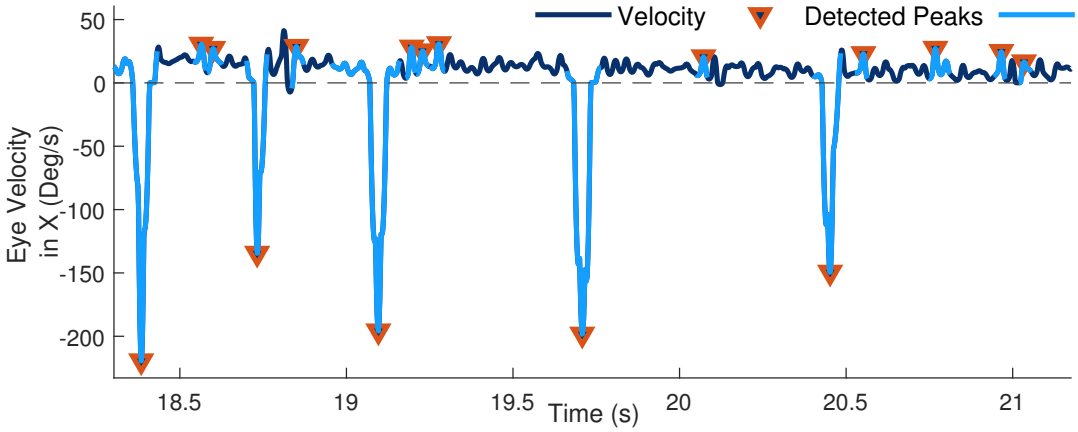

Figure 5.6: Peak selection Selected peaks according to R_2 and their periods

5.3 Clustering

5.3.1 Feature Extraction

Different features are computed for each of the selected peaks (described in appendix). Feature selection was performed initially using Spearmann Correlation Coefficient matrix, Dunn's index and Random Forest. Based on the results of these different methods, three features were selected:

- Prominence of the peak computed as maximum height of the peak from baseline (*prom*)
- Difference between peak and median of eye velocity 100ms before/ after peak to signify noise level around the peak (*meddiff_vel*)
- 1st level decomposition co-efficients of discrete wavelet transform (using 10th order Daubechies wavelet, db10, due to its close overlap with a Gaussian shape) of the velocity at the location of selected peaks (*wv*)

Logarithm is then applied on the absolute of the extracted feature values. This is done to make the feature distribution approximating Gaussian and reduce the skewness and the heavy tails of their distributions. Each of the 3 features are then normalized using zscoring which brings the mean of each type of feature to zero and the standard deviation to 1 as shown below:

$$z = \frac{f_i - \mu}{\sigma}$$

where z is the zscore of feature value f_i, while μ and σ are the mean and standard deviation of the distribution of feature respectively.

5.3.2 Spectral Clustering

Data points with similar properties (here, features) group together to form clusters. Identifying data points belonging to such clusters is referred to as clustering. Clustering is one of the most widely used unsupervised Machine Learning techniques in data analysis for applications ranging from biology, computer science to psychology and commercial marketing.

K-means is one of the traditional clustering algorithms in which distances from data points to an initial K chosen points (centroids) are computed iteratively and all the data points are assigned to their respective nearest centroids to form K clusters. Centers of these K clusters are then recalculated and updated iteratively. The goal of K-means is thus to decrease the distance between data points in a cluster. However, this technique is susceptible to erroneous results in the presence of low density clusters and not able to detect non-spherical clusters (Jain, 2010).

To address this shortcoming, Rodriguez and Laio, 2014 proposed a density based clustering method. This approach includes the calculation of distances between each data point which are then used to compute density (ρ_i) of each point using a Gaussian kernel. Clusters are then identified by thresholding the distance (γ_i) of each point to its nearest point with higher density. This threshold distance can be obtained in different ways. Sheynikhovich et al., 2018 first applied this method on eye tracking data for microsaccade detection by using a *k*-dist graph for finding the threshold distance. However, application of this method on the current data (Punuganti, Tian, and Otero-Millan, 2019) did not yield satisfactory results due to problems in choosing a threshold distance.

Moreover, in order to form tighter clusters, the extracted features from previous step have to be represented in a different dimension. Thus, **spectral clustering** was chosen in the present study. This method has shown to outperform traditional clustering approaches and is also easy to implement. The name of this method is derived from **spectrum of a matrix**, which refers to the set of the matrix's eigenvalues.

The main tool needed for spectral clustering is the graph Laplacian matrix, from the field of spectral graph theory (Luxburg, 2007). Data points can be represented in the form of a *similarity graph*, $G = (F, E)$, where F is the set of data points (here, feature vectors) $f_1, ..., f_n$ and E represents the set of edges between each of these data points. An edge between two data points (also called as vertices of the edge) f_i and f_j is weighted by the similarity, s_{ij} between them. And the two points, f_i and f_j are said to be connected if s_{ij} is positive or larger than a threshold. The aim of spectral clustering is then to find a partition of the graph such that edges between clusters have low weights. Though there are many algorithms proposed for performing spectral clustering, the following method proposed by (Ng, Jordan, and Weiss, 2002) is one of the most commonly employed methods.

A graph should represent local neighborhood relationships of the feature vectors and this can be done by weighing the edges using a similarity function that itself models local neighborhoods. In the present study, the edges are weighted using a Gaussian similarity function, $s(f_i, f_j) = exp(-\|f_i - f_j\|^2/2\sigma^2)$, where σ controls for the width of the overlapping neighborhood between data points.

We can see that $s_{ij} \geq 0$ and if $s_{ij} = 0$, then f_i and f_j are not connected by an edge. This type of graph is called as ***fully connected graph*** and it is an ***undirected graph*** since $s_{ij} = s_{ji}$. The ***weighted adjacency matrix***, S, of the graph and degree of a data point, d_i are respectively defined as:

$$S = (s_{ij})_{i,j=1,...,n}$$

$$d_i = \sum_{j=1}^{n} s_{ij}$$

The ***degree matrix*** D is diagonal matrix of all the degrees (with $d_1, ..., d_n$ on the diagonal). The normalized graph Laplacian (which is also symmetric), L, is now defined as:

$$L = D^{-1/2} L D^{-1/2}$$

Eigenvectors of L are then computed as below:

$$Lu = \Lambda u$$

where Λ consist of the eigenvalues. The first k eigenvectors, $u_1, ...u_k$ L are then normalized to form clusters. If $k > 2$, then K-means clustering is applied to this representation of the original data points in order to find the k clusters. However, in the present study $k = 2$, corresponding to cluster formed by actual QPs and that by noise peaks. These two clusters are separated by a threshold of 0.

For the present study, any value of σ greater than 3 did not produce considerable differences in the results, hence a value of 3 was chosen for this parameter. Figure 5.7 represents the feature vectors using Multi-Dimensional Scaling (MDS), which is a tool that aids in data visualization. The quick phases

were manually labeled using a MATLAB labeling tool by the author. As can be seen, the points corresponding to true quick phases are highly correlated due to their high velocity, whereas the noise points are scattered without any correlation. Figure 5.8 shows detected QPs in the eye position trace.

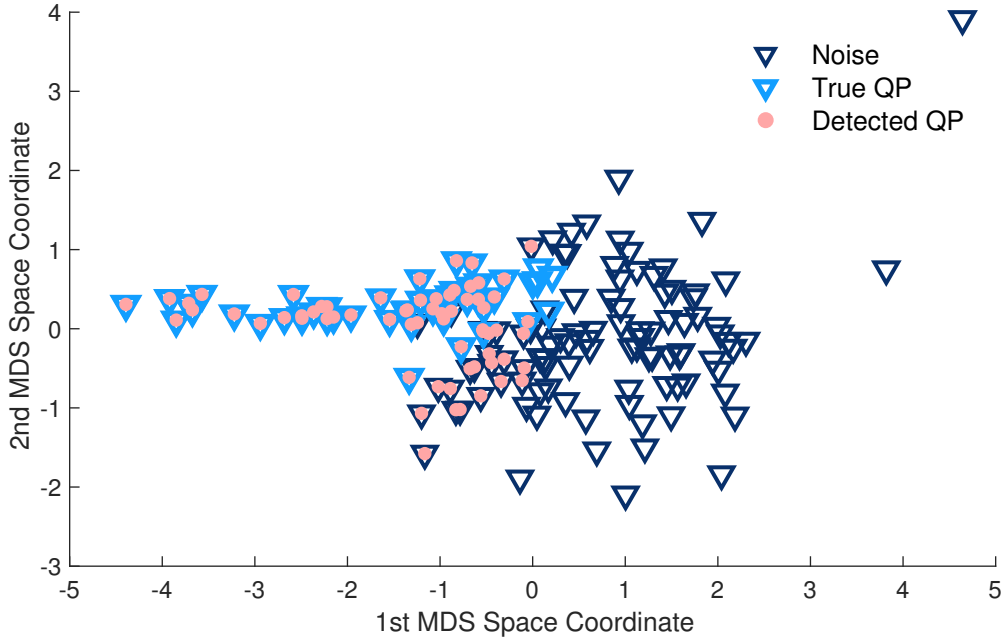

Figure 5.7: MDS of feature vectors showing detected QPs

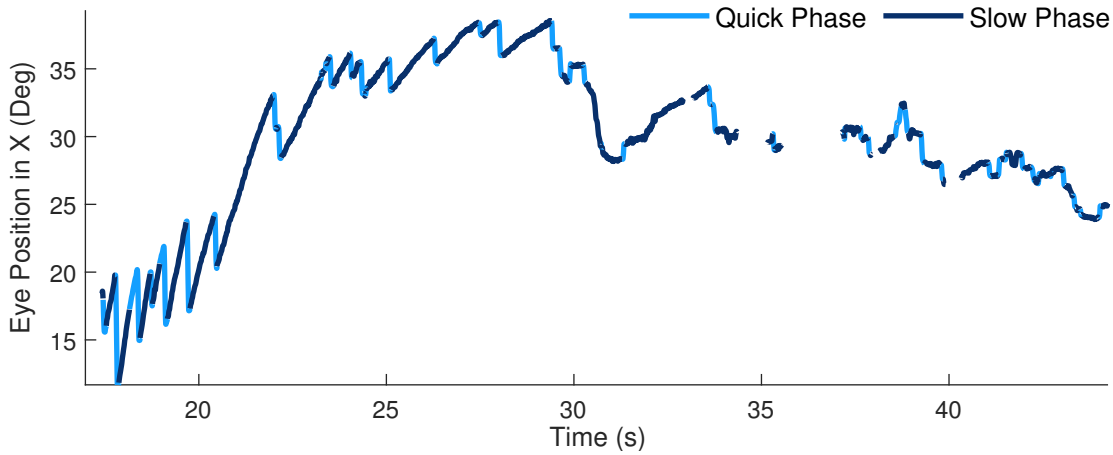

Figure 5.8: Detected QPs in the eye position signal

5.4 Slow Phase Velocity Estimation

Saccades or quick phases detected from the above step are removed from the cleaned and resampled velocity signal (i.e., non-smoothed). The resulting velocity signal represents periods of non-saccadic eye movements. This signal is median filtered using a window of 1s, taking care that missing data (representing the removed bad data) do not propagate (smoothed SPV in Figure 5.9). From this filtered signal, median Slow Phase Velocity (SPV) within each window of 1s is obtained to get final estimate of SPV signal (Figrure 5.10).

The position of maximum SPV value is then determined. Samples from either side of this maximum value are averaged (this amounts to averaging median SPV in window of 3s). However, if both of the samples before and after the maximum SPV are opposite in sign to the maximum SPV, then then next maximum SPV is found. This is done since for a recording with nystagmus, direction of slow phases should not change direction within 1s.

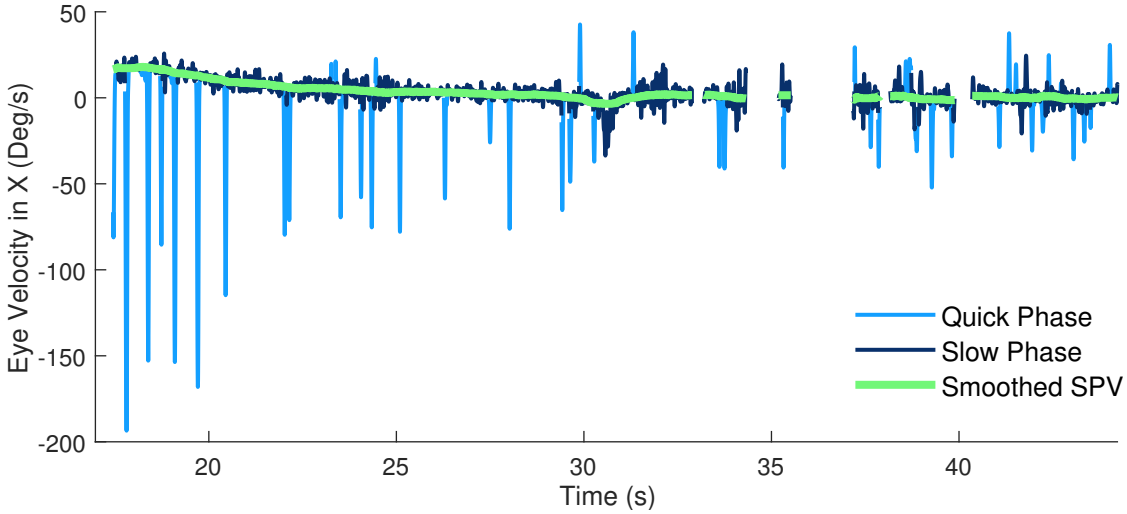

Figure 5.9: Smoothed SPV Estimate of slow phase velocity

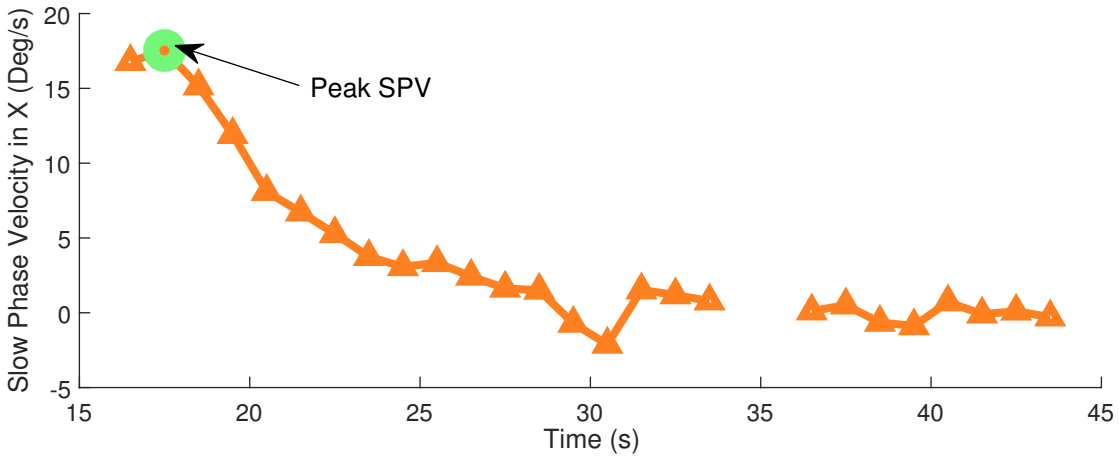

Figure 5.10: Peak SPV detected from the final SPV trace

5.5 Algorithm Overview

An overview of each of the steps described in the above proposed custom algorithm is given below. All the thresholds, windows and parameters used in the current method are listed in Appendix A.

Algorithm Nystagmus Detection

procedure DATA PRE-PROCESSING(x, y, t)
    Clean & *resample* eye position data to 500Hz
end procedure
Output: X, Y, T

procedure PEAK DETECTION & SELECTION(X, Y, T)
    for $pos = [X, Y]$ **do**
        $v \leftarrow \frac{d(pos)}{dT}$ ▷ Raw velocity
        $vel \leftarrow \texttt{Smooth}(v)$ ▷ Smoothed velocity
        $peaks.loc \leftarrow$ Find local maxima (peaks) in vel^2
        $[peaks.start, peaks.stop] \leftarrow$ find start & stop of each peak
        $peaks.prom \leftarrow$ Find prominence of each peak
        $r \leftarrow MAD(peaks.prom)$
        $R_1 \leftarrow peaks.prom > r$

$R_2 \leftarrow R_1 \times F$
$peaks \leftarrow R_2$ peaks/s
end for
end procedure
Output: *peaks* ▷ Selected peaks in X & Y

procedure CLUSTERING(*peaks*)
for $data = [peaks.X, peaks.Y]$ **do**
$f \leftarrow$ Extract features from *data* ▷ Features
$f \leftarrow \texttt{zscore}(\log(|f|))$ ▷ Normalized features
$S \leftarrow s_{ij} = e^{\frac{-\|f_i - f_j\|^2}{2\sigma^2}}$ ▷ Weighted adjacency matrix
$D \leftarrow d_{ij} = \sum_{j=1}^{n} s_{ij} \; \forall \; i = j$ ▷ Diagonal degree matrix
$L = D^{-1/2} L D^{1/2}$ ▷ Graph Laplacian
$u \leftarrow$ First 2 eigenvectors of L
$U \leftarrow U_{ij} = \frac{u_{ij}}{\sum_{j=1}^{n} u_{ij}^2}$ ▷ Normalized eigenvectors
$labels = U \geq 0$
end for
end procedure
Output: *labels* ▷ Cluster labels

procedure SPV ESTIMATION($X, Y, labels$)
for $pos = [X, Y]$ **do**
$v \leftarrow$ Remove QPs using *labels*
$spv \leftarrow$ Median filter v
$spv \leftarrow$ Median of spv in each s
$i \leftarrow$ location of max spv
while $spv_{i-1} \times spv_i == 1$ || $spv_{i+1} \times spv_i == 1$ **do**
$SPV \leftarrow mean[spv_{i-1}, spv_i, spv_{i+1}]$
end while
end for
Output: SPV_X, SPV_Y ▷ SPV estimate for X & Y

Chapter 6

Results

The proposed method was applied to the 157 eye movement recordings of the Dix-Hallpike (left and/or right) tests recorded using the ICS Impulse Otosuite^{TM} software in the AVERT study, recorded from 103 patients. Using the manual labeling of each of these tests for positive/ negative nystagmus outcome (as shown in Table 6.1), results from the custom algorithm were compared against those from the Otosuite^{TM} software using two methods:

1. Receiver Operating Characteristic (ROC) curves
2. Diagnostic test measures

Both the methods provide an output corresponding to the two components of the eye movements (horizontal (X) and vertical (Y) components). Our custom algorithm outputs either an SPV value for the component or SPV **undefined** that indicates that data is too corrupted to be able to output any result. The Otosuite^{TM} software outputs either an SPV value for the component or a value of 9999 that indicates that no nystagmus was identified. In these cases where Otosuite^{TM} outputs 9999, the SPV value is taken as zero for the corresponding component of the eye movement recording.

Out of the 314 recordings, the custom algorithm was unable to calculate the SPV in 26 recordings, and thus gave a result of SPV **undefined**. These 26 recordings comprised of 13 horizontal and 13 vertical cases.

	Total	X	Y
Eye Recordings	314	157	157
Positive Nystagmus	39	23	16

(a)

	Total	X	Y
Eye Recordings	288	144	144
Positive Nystagmus	37	22	15

(b)

Table 6.1: Eye recordings Table (a) shows composition of the total number of eye recordings while Table (b) shows that of the recordings from which bad cases detected by custom algorithm are removed (X - Horizontal and Y - Vertical components)

Computation time of custom algorithm ranges from 0.8s (for a 11s recording) to 18.5s (for a 124s recording) on a normal desktop computer (16GB, 3.2 GHz Intel Core i7-8700). These timings are computed for the entire algorithm that includes the four stages.

6.1 Analysis of ROC Curves

Receiver Operating Characteristic (ROC) curve was developed during World War II for measuring the ability of Radar to detect enemy objects on battlefield. It has been adapted since then into various fields for assessment purposes.

A binary classifier can be assessed using the ROC curve by thresholding the output of the classifier. The ROC curve plots the true positive rate against the false positive rate obtained after the resulting values output by the classifier are thresholded at different values. The classifier output values in this case are the Slow Phase Velocity (SPV) values output by the algorithm. The ROC curve is thus used to assess how accurately can the algorithm detect a nystagmus case as the threshold on the estimated SPV output by the algorithm is varied.

The area under the ROC curve (also called as Area Under Curve (AUC)) is a statistic that is used to interpret the performance of the classifier. Many fields use this parameter for model comparison. It quantifies the capability of a diagnostic test to distinguish between positive and negative cases.

Figure 6.1 shows the ROC curve obtained for custom algorithm against Otosuite^{TM} software. This curve shows combined result of X and Y components for a total of 288 recordings. As can be seen, the Area Under Curve (AUC) obtained for the custom algorithm for both horizontal and vertical components combined is 95% which is higher than the AUC of Otosuite^{TM} which was obtained as 89%.

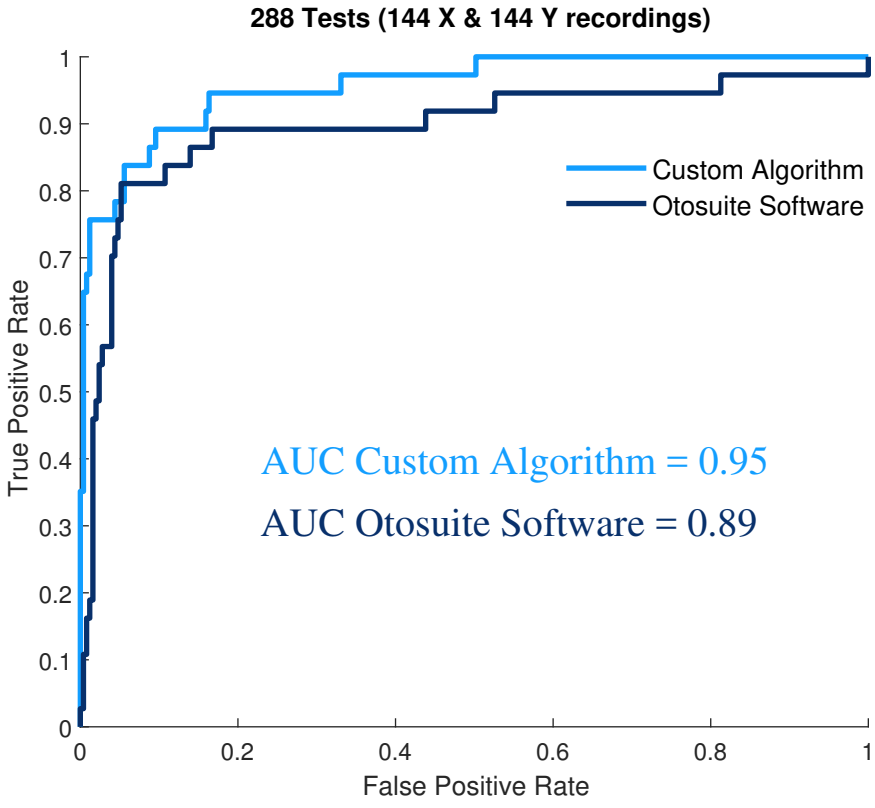

Figure 6.1: ROC curves for both horizontal and vertical tests

Figure 6.2 shows the ROC curve obtained for custom algorithm and the Otosuite^{TM} software when applied on only the 144 horizontal recordings. Though the most common form of BPPV involves vertical/torsional nystagmus, in the present study there were more positive cases in the horizontal component than in the vertical component. This can be attributed to the inclusion of non-BPPV patients who might have showed nystagmus due to conditions other than BPPV. As before, even in the case of horizontal components only, the AUC obtained for the proposed custom algorithm is at 95%, while it is at 90% for the Otosuite^{TM} software.

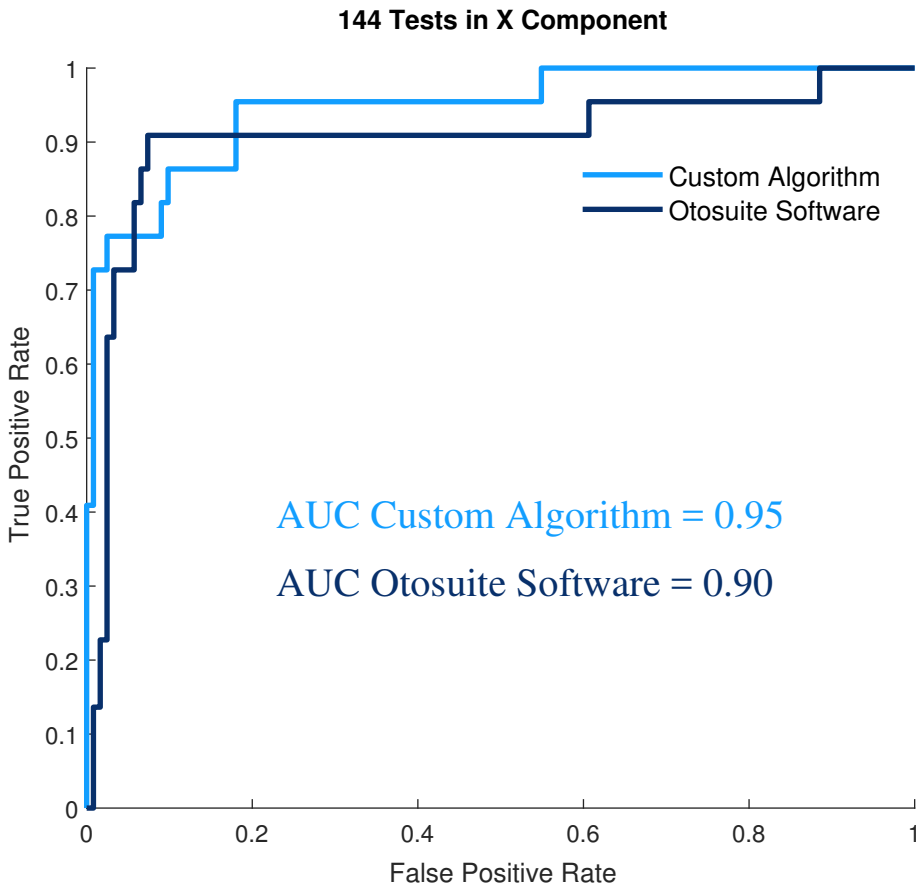

Figure 6.2: ROC curve for hrizontal tests

Similarly, Figure 6.3 shows the ROC curve obtained for custom algorithm and the Otosuite^{TM} software when applied on only the 144 vertical eye movement recordings. Number of positive nystagmus cases in vertical component are generally lower than in horizontal component. In case of vertical component of eye recordings only, AUC for custom algorithm was obtained as 97% while Otosuite^{TM} resulted in an AUC of 88%.

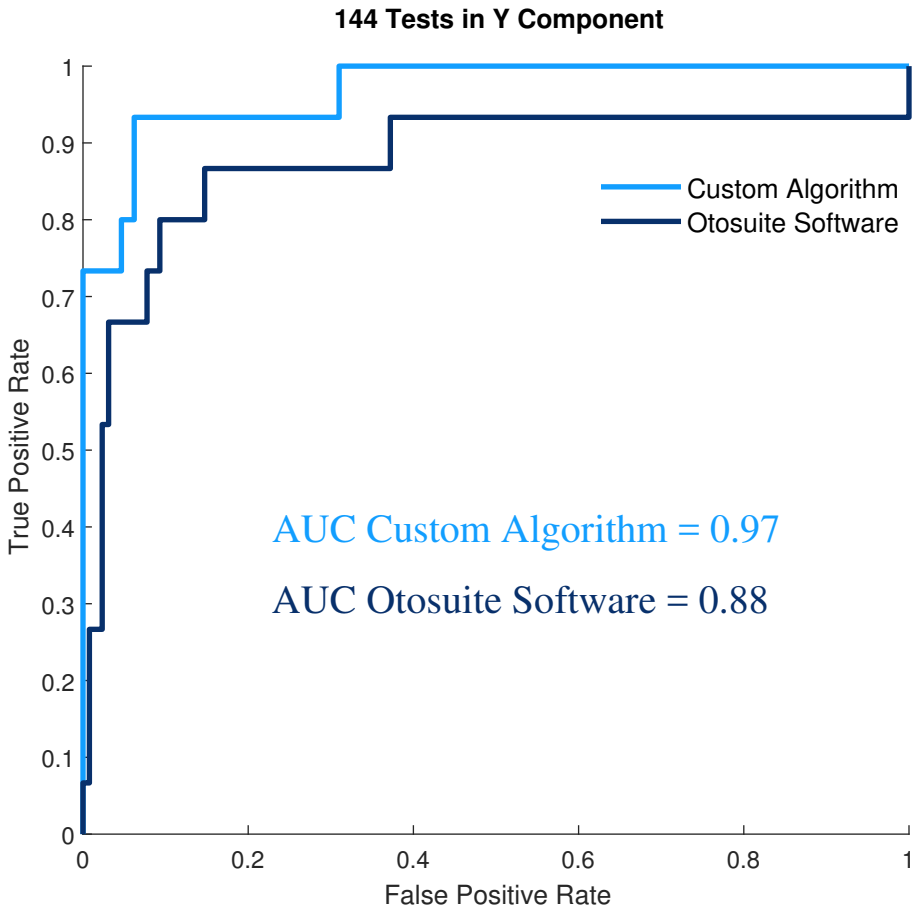

Figure 6.3: ROC curve for vertical tests

Figure 6.4 shows the ROC curve for Otosuite^{TM} when applied on the 26 cases for which custom algorithm gave an output of SPV **undefined**. It can be

seen that Otosuite^{TM} gives almost random output in these bad cases as per its AUC which is at 47%. Figure 6.5 represents an example recording where the custom algorithm gives an output of SPV **undefined**. It can be seen that the signal is corrupted and it is impossible to output a result in this recording.

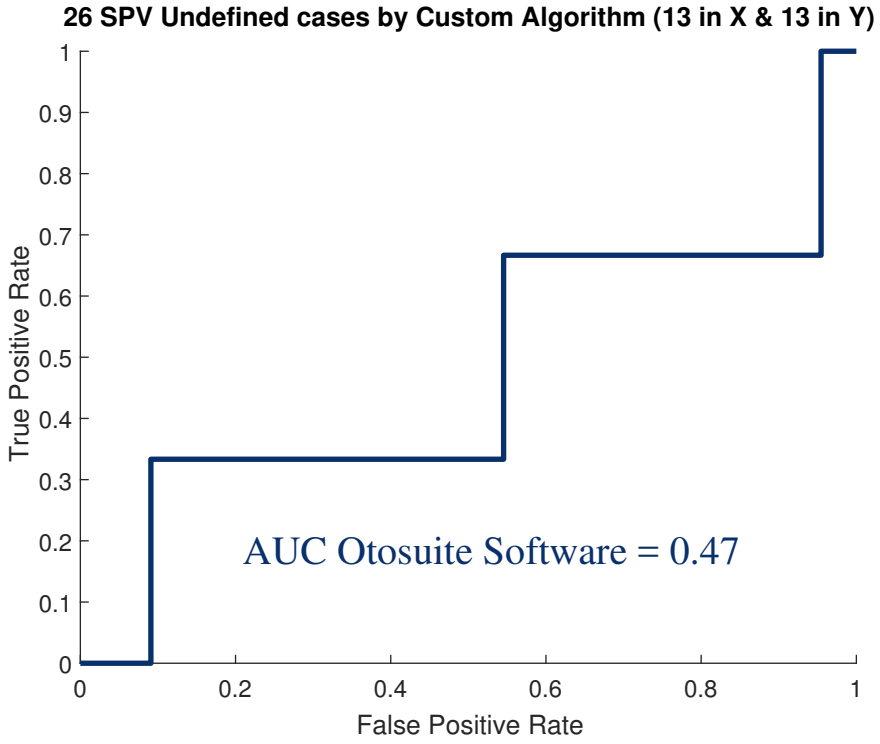

Figure 6.4: ROC curve of Otosuite^{TM} on cases of SPV **undefined** by custom algorithm

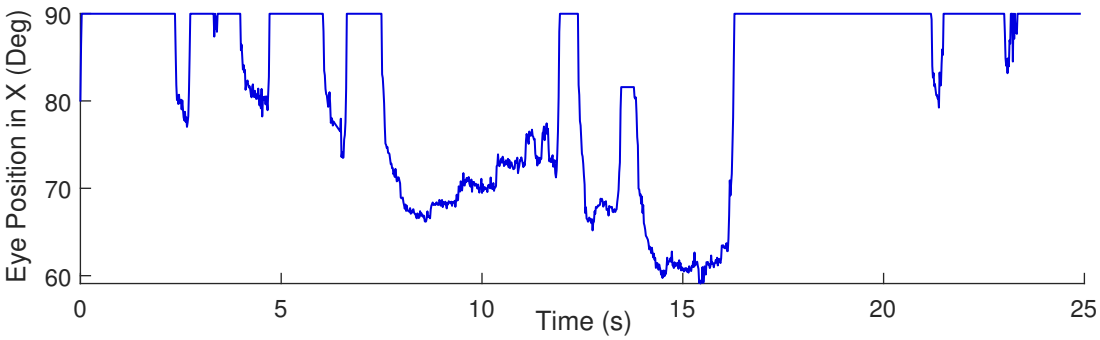

Figure 6.5: Undefined case by custom algorithm Example of highly corrupted recording detected by custom algorithm where no SPV could be calculated

Figures B.2 shows an example eye recording from a patient with nystagmus. A clear pattern of alternating quick phases and slow phases can be seen from the nystagmus recording. Figure 6.7 shows eye movement recording from a patient without nystagmus on the same time scale and degree scale as Figure B.2. There are clear saccades being made but there is no slow phase (i.e., no slow eye drift) in between the saccades. Consequently, the recording with nystagmus is expected to have a higher SPV and the one without nystagmus a lower estimate of SPV.

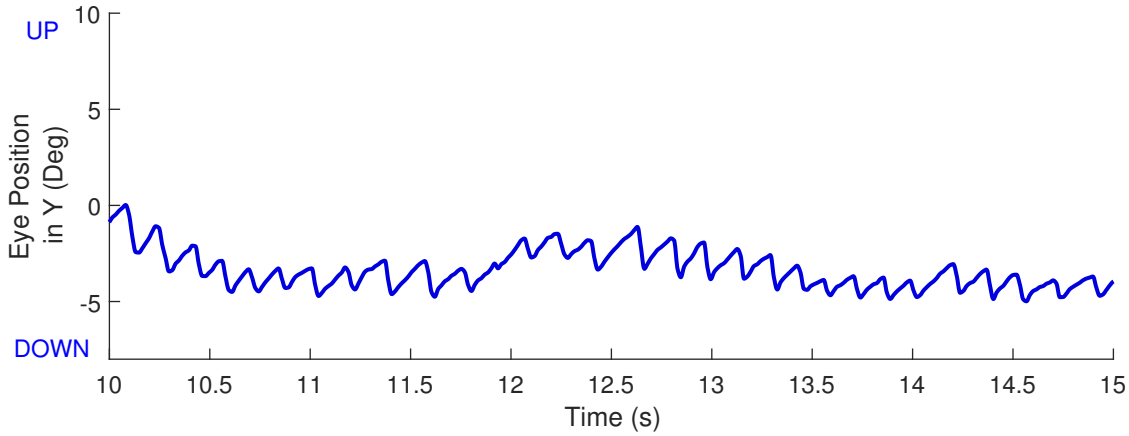

Figure 6.6: Eye recording from patient with nystagmus

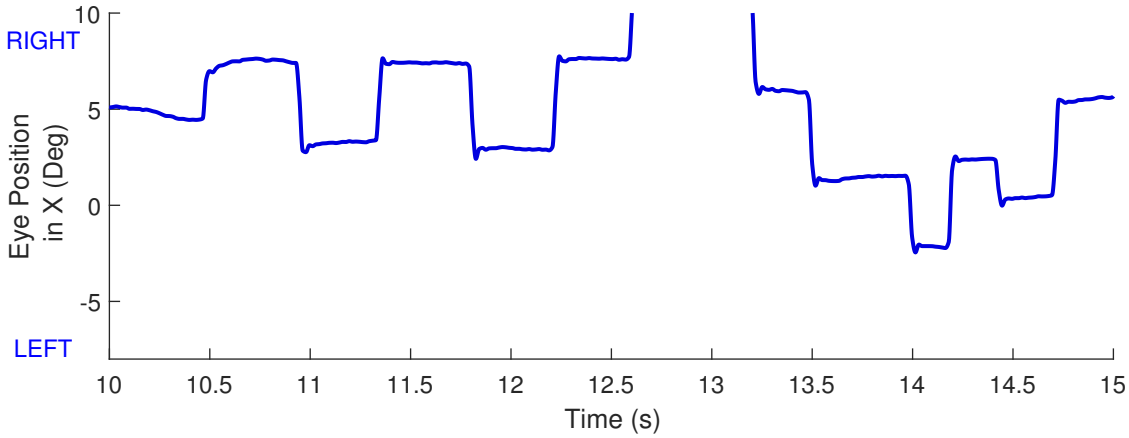

Figure 6.7: Eye recording from patient without nystagmus

The resulting SPV obtained from the custom algorithm for the above two examples are shown in Figures 6.8 and 6.9 respectively. The SPV for the recording with nystagmus (Figure B.2) can be seen to be high, at about $10^o/s$ from Figure 6.8. And as expected, the SPV of the recording without nystagmus (Figure 6.7) can be seen to lower, near to $0^o/s$ in Figure 6.9.

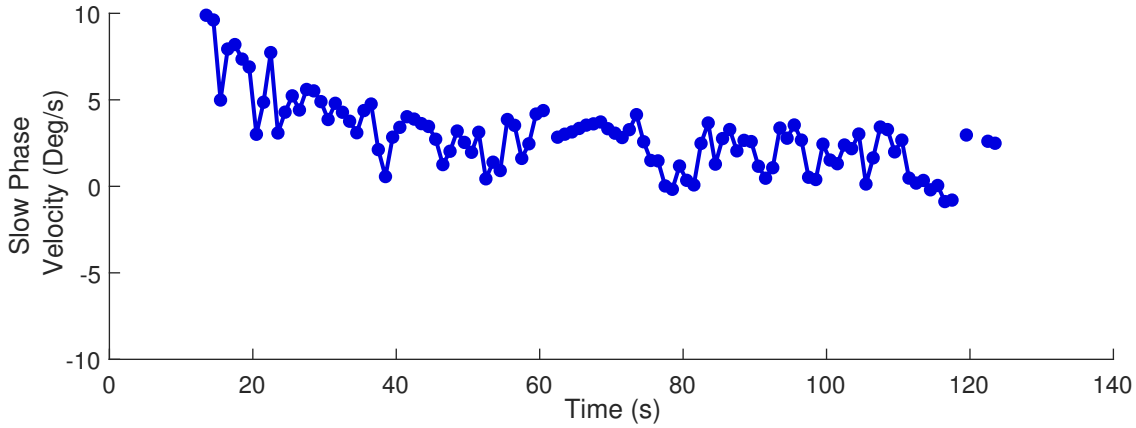

Figure 6.8: SPV of eye position in figure B.2 with nystagmus

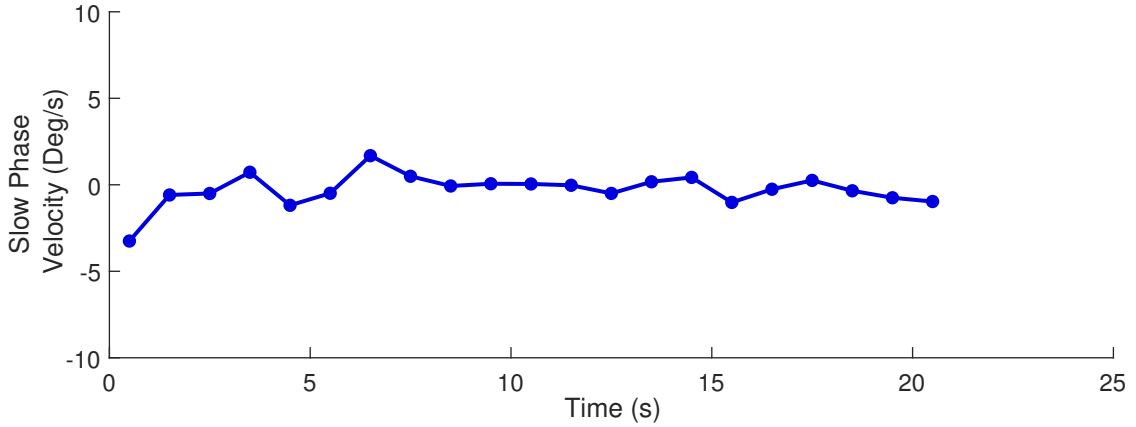

Figure 6.9: SPV of eye position in figure 6.7 without nystagmus

6.2 Analysis of Diagnostic Test Measures

The efficacy and accuracy of a medical test can be measured by four parameters as will be described below. Here test specifically refers to the diagnostic tool used in the diagnosis. In our case, the proposed custom algorithm and the commercial Otosuite^{TM} software are the tests being compared.

- **Sensitivity** of a test is defined as the probability of the test to identify positive cases among those with the disease.

$$Sensitivity = \frac{TP}{TP + FN}$$

- **Specificity** of a test is defined as the probability of the test to identify negative cases among those without the disease.

$$Specificity = \frac{TN}{TN + FP}$$

- **Positive Predictive Value (PPV)** is the probability that patient with a positive test result truly has the disease.

$$PPV = \frac{TP}{TP + FP}$$

- **Negative Predictive Value (NPV)** is the probability that patient with a negative test result truly does not have the disease.

$$NPV = \frac{TN}{TN + FN}$$

where, TP = True Positives, FP = False Positives, TN = True Negatives & FN = False Negatives

6.2.1 Both Horizontal & Vertical Recordings

Sensitivity and specificity for custom algorithm when applied on the 314 recordings was found to be at 89% and 86% respectively (Table 6.2). This does not change when applied on the 288 recordings that exclude the **undefined** cases. Otosuite^{TM} achieves a sensitivity of 89% but a lower specificity of 55%. Also, Otosuite^{TM}'s sensitivity increased to 92% (while specificity remained the same at 55%), when applied on the 288 recordings that exclude corrupted recordings detected by custom algorithm (Table 6.3). These values are obtained at a threshold of $5^{o}/s$.

PPV and NPV for custom algorithm are found to be 92% and 95% respectively (Table 6.2). While for Otosuite^{TM}, PPV was found to be at 70% and NPV at 97% when applied on the complete set of recordings (314 signals). These values are obtained at a threshold of $10^{o}/s$. This shows that custom algorithm performs better in general as both the PPV and NPV are satisfactory (above 90%) whereas Otosuite^{TM} has a low PPV even though it has a high NPV.

	Sensitivity	Specificity	PPV	NPV
Custom Algorithm	89	86	92	95
Otosuite^{TM}	89	55	70	97

Table 6.2: Test measures obtained on 314 (157 in each of X and Y) that includes bad cases detected by algorithm (All values are in percentage)

	Sensitivity	Specificity	PPV	NPV
Custom Algorithm	89	86	92	95
Otosuite^{TM}	92	55	70	97

Table 6.3: Test measures obtained on 288 (144 in each of X and Y) that excludes bad cases detected by custom algorithm (All values are in percentage)

6.2.2 Only Horizontal Recordings

Sensitivity and specificity for custom algorithm when applied on the 157 horizontal recordings was found to be at 86% and 84% respectively (Table 6.4). Otosuite^{TM} achieves a sensitivity of 91% but a low specificity of 49%. These values are obtained at a threshold of $5^{o}/s$.

PPV and NPV for custom algorithm are found to be 89% and 95% respectively (Table 6.4). While for Otosuite^{TM} PPV was found to be at 60% and NPV at 97%. These values are obtained at a threshold of $10^{o}/s$. This shows that custom algorithm performs better in general as all the four measures are satisfactory (above 80%) whereas Otosuite^{TM} has lower specificity and PPV (below 60%) even though it has a high sensitivity and NPV. Also, Otosuite^{TM}'s PPV increased to 69% (while specificity and sensitivity remained the same at 49% and 91% respectively), when applied on the 144 recordings that exclude corrupted recordings detected by custom algorithm (Table 6.5).

	Sensitivity	Specificity	PPV	NPV
Custom Algorithm	86	84	89	95
Otosuite^{TM}	91	49	60	97

Table 6.4: Test measures obtained on 157 horizontal only recordings that includes bad cases detected by algorithm (All values are in percentage)

	Sensitivity	Specificity	PPV	NPV
Custom Algorithm	86	84	89	95
Otosuite^{TM}	91	49	69	98

Table 6.5: Test measures obtained on 144 horizontal only recordings that excludes bad cases detected by custom algorithm (All values are in percentage)

6.2.3 Only Vertical Recordings

Sensitivity and specificity for custom algorithm when applied on the 157 vertical recordings was found to be at 93% and 88% respectively (Table 6.6). Otosuite^{TM} achieves a sensitivity of 88% but a low specificity of 60%. Also, Otosuite^{TM}'s sensitivity increased to 93% (while specificity remained the same at 60%), when applied on the 144 recordings that exclude corrupted recordings detected by custom algorithm (Table 6.7). These values are obtained at a threshold of $5^{o}/s$.

PPV and NPV for custom algorithm are found to be 100% and 95% respectively (Table 6.6). While for Otosuite^{TM} PPV was found to be at 63% and NPV at 96%. These values are obtained at a threshold of $10^{o}/s$. This shows that custom algorithm performs better in general as all the four measures are satisfactory (above 85%) whereas Otosuite^{TM} has lower specificity and PPV (below 65%) even though it has a high NPV.

	Sensitivity	Specificity	PPV	NPV
Custom Algorithm	93	88	100	95
Otosuite^{TM}	88	60	63	96

Table 6.6: Test measures obtained on 157 vertical only recordings that includes bad cases detected by algorithm (All values are in percentage)

	Sensitivity	Specificity	PPV	NPV
Custom Algorithm	93	88	100	95
Otosuite^{TM}	93	60	71	96

Table 6.7: Test measures obtained on 144 vertical only recordings that excludes bad cases detected by custom algorithm (All values are in percentage)

Although details of the algorithm employed by Otosuite^{TM} are unknown, some of the false positive cases output by Otosuite^{TM} can be attributed to the peak SPV being detected during artifacts, periods of head movement or during patient drowsiness. However, periods of patient drowsiness sometimes also cause false positives in the custom algorithm. As discussed earlier, Otosuite^{TM} also fails to detect recordings with very bad data (e.g., Figure 6.5), which also contribute to some of the false positives. In few true positive cases, Otosuite^{TM} detected the peak SPV at a point where there is no nystagmus, leading to outputs that are by fluke in such cases.

Chapter 7

Discussion

7.1 Summary

Even though BPPV is found to be the most common cause of vertigo/ dizziness, patients presenting with dizziness and vertigo to the Emergency Department (ED) have a high chance of being misdiagnosed (43%). BPPV can be treated as well as diagnosed using simple maneuvers done by experts. During the diagnostic maneuver, a patient with BPPV shows nystagmus (an involuntary eye condition comprising of alternating saccades/QPs and slow phases). Using VOG goggles to record patient's eye movements, this condition can be automatically diagnosed.

Automatic medical diagnosis can aid the ED practitioners in making better diagnosis. However, currently employed system for nystagmus detection in patients, the ICS Impulse Otosuite^{TM}, is found to have low specificity (Chang et al., 2019). Thus, proposed algorithm aims to improve current state of automatic nystagmus detection, thereby contributing to automatic medical diagnosis of dizzy patients and address the issue of high rate of misdiagnosis.

From our results, it can be seen that proposed algorithm performs better than Otosuite^{TM} in detecting nystagmus when applied on 314 patient recordings from 103 patients. ROC curves show superior performance of custom algorithm compared to the Otosuite^{TM} (Figures 6.1 - 6.4). With diagnostic test measures (sensitivity, specificity, PPV and NPV) having higher values than Otosuite^{TM} overall (Tables 6.2 - 6.7) conveying higher accuracy of nystagmus detection by the proposed algorithm compared to Otosuite^{TM}, which tends to produce more false positives.

The peak SPV corresponding to the nystagmus due to BPPV in the different canals can fall into different velocity ranges. While there are reports of BPPV patients showing SPV as low as $4^o/s$ (Han, Oh, and Kim, 2006) in their nystagmus, in general, an SPV threshold of $5^o/s$ resulted in better sensitivity and specificity measurements for the present study. However, the ROC curves (in Figures 6.1 - 6.3) are not limited to this threshold of $5^o/s$, as they represent the overall performance of the algorithm at different threshold values.

The proposed algorithm first identifies and removes the quick phases after which an SPV estimate is obtained for quantifying the intensity of nystagmus in the patient. Quick phases are generated by the same mechanisms as that saccades, and hence this algorithm can also be used for saccade detection.

No prior user experience or user training is necessary for employing the current algorithm. The proposed algorithm is modular, comprising of four stages: preprocessing, peak detection and selection, clustering and SPV estimation. Each module can be improved independently, if the user chooses to. Changing one stage will not affect the subsequent stages.

The proposed method employs a two-pass system for identifying saccades in comparison to the traditional saccade detection algorithms. Overall velocity peaks are detected and subsequently a subset of them are chosen based on a computed threshold. Peak selection involves the use of rate factor based on the physiological observation that rate of saccades is limited to 1-6 per second. The peak selection ensures that data points are balanced and possess the capacity to form clusters, thus aiding in the subsequent clustering stage. As can be seen, this is a novel top-down approach that is robust, easy to understand and implement and unsupervised.

In supervised learning, recent years has seen steady increase in the use of neural networks or artificial intelligence for purposes of medical diagnosis. As discussed in chapter 3, various neural networks have been developed for eye movement detection on eye tracking data. For one thing, comparison between the different proposed neural networks has not yet been achieved. Further, application of these networks require laborious and time-consuming manual labeling of data as they depend on the type of eye tracker used to collect the data. Current widely used CNN architectures cater to high dimensional data and hence neural networks have been successful for images i.e., multi-dimensional inputs. However, successful networks for accurate classification of 1D signal are yet to be designed.

Clustering is chosen since it is an unsupervised method and has the promise of robust classification. Clustering techniques do not require model training and are not dependent on the type of eye tracker used for data collection. Most importantly, they do not require user training. In the present study,

Spectral Clustering was chosen for classifying the selected peaks.

Recently developed density based clustering methods are sensitive to parameters and are highly dependent on the scale of features whereas spectral clustering is not. Traditional clustering algorithms involve use of euclidean distance metrics to measure similarity between data points. These types of distance metrics assume a convex shape to the underlying clusters and hence traditional clustering algorithms would not yield good results. Spectral clustering is evolved to find complex clusters in different shapes such as intertwined spirals, non-linear or other complex structures. Whereas traditional methods such as K-means and generative models fail to identify such type of complex clusters. Moreover, traditional probabilistic clustering algorithms (e.g., mixture models) involve Expectation Maximization step that needs to have multiple starting points in order to reach the ideal minima.

Current method does not combine horizontal and vertical components and this arises from the fact that nystagmus can occur in either component, independent of the other. However, this separation of components is also advantageous compared to when methods that combine them since the peak velocity of a saccade can differ by few samples in these two components. This difference in location of saccade peak velocity generally arises from errors in data acquisition and it can be exacerbated by filtering or other signal processing techniques. This in turn affects the detected beginning and ending points of the saccade. Thus, it is better to find saccades and their duration in the relative time reference of the respective components rather than combining them.

Bed-side VOG recordings from patients are highly susceptible to artifacts and different kinds of noise. Most proposed algorithms are typically useful for laboratory settings where eye movement data is recorded under controlled conditions resulting in data that is comparatively very low in artifacts and noise. The fact that current algorithm is able to detect quick phases (which are nothing but saccades) in non-ideal conditions from patients while being able to provide accurate detection of nystagmus is promising.

A key feature of the current algorithm is its ability to identify bad eye movement recordings that are corrupted with artifacts/ noise to such an extent that it is impossible to provide an outcome even manually. In such cases, Otosuite^{TM} gives an almost random output as can be seen by the AUC of its ROC curve, in Figure 6.4, when applied on the 26 cases which were detected as bad eye recordings by the custom algorithm.

However, in some cases present algorithm fails to detect few apparent saccades even though saccades with lower amplitude are detected. This could be due to the feature engineering. Feature selection needs to be looked into in future studies on eye movement detection algorithms. Also, current algorithm would give false positives in high noise eye movement recordings having zero to very few saccades. This can be attributed to the top-down approach used for the proposed method. Additionally, detection of periods when patient becomes drowsy would be highly useful, especially in nystagmus detection as these periods can lead to a high SPV estimate.

Below is a summary of the salient points of the proposed method:

1. Separated analysis of horizontal and vertical components ensures robust saccade onset and offset detection
2. Algorithm is modular, ensuring that different stages can be improved independently
3. No user training or user experience is necessary for implementation
4. Novel top-down approach and peak selection using rate factor ensures balanced dataset for clustering
5. Unsupervised method: Clustering does not require any data training or labeled dataset
6. Two-pass system for saccade detection
7. Can be applied to dynamic as well as static tasks
8. Ability to detect corrupted recordings of data (can distinguish bad data from good data)
9. Good results even in non-ideal data collection settings: bedside recordings from patients are susceptible to more noise and artifacts than controlled laboratory conditions.
10. Most of the thresholds are based on physiological parameters

7.2 Future Work

Future steps for the present study of developing a robust nystagmus detection method are as detailed below:

1. Procedure for detection of periods when patient is drowsy.

2. Validation of present algorithm on eye movement data recorded from other eye trackers.

3. Comparison with current state-of-the-art saccade detection algorithms.

4. Integration of the proposed algorithm with other automatic medical diagnostic algorithms.

Appendix A

Algorithm Variables

A.1 Thresholds

Threshold	Value	Setting
Data Pre-processing		
Eye position	1000^o	When eye position is out of range
Eye Velocity	$500^o/s$	When eye velocity is out of range
Acceleration	$50000^o/s^2$	When acceleration is out of range
Head velocity	$10^o/s$	When patient's head is moved during diagnosis
Saccade rate	15	Physiological limit of max saccades/s in humans
Velocity (for detecting software artifacts)	$25^o/s$	To detect software artifacts due to eyelashes or loss of pupil center
Peak Detection and Selection		
Percentage of highest velocities	5	To estimate initial SPV baseline
Inter-saccadic interval	$30ms$	Physiological limit
Minimum peak threshold	$20^o/s$	Minimum eye velocity threshold to select peaks

Maximum threshold	$50^o/s$	Maximum eye velocity threshold to select peaks
Minimum R_2	3	Minimum number of saccades/s during free viewing
Maximum R_2	15	Maximum number of saccades/s for humans

Table A.1: Thresholds Different thresholds, their values and settings used in the algorithm. Most of these thresholds are based on physiology of human eye movements and are hence true for eye recordings.

A.2 Windows

Window	Value	Setting
Data Pre-processing		
Interpolable missing frames	3	Maximum consecutive number of missing frames to interpolate
Flat periods	3	Consecutive samples that are equal in value
Removal of artifacts	200ms	Total number of peaks within this window indicate presence of artifacts/ spiky data
Interpolable spikes	1	One-sample spikes in between good data can be interpolated
Bad data padding	200ms	Padding of data to be removed around the detected bad data
Head velocity padding	400ms	Padding of data to be removed around head movement
Peak Detection and Selection		
Smoothing velocity	5	Number of velocity samples to average over for decreasing noise

Start/end point detection (or period detection)	300ms	Window before/ after a peak to search in for its start/ end points
Peak selection window	1s	Window to select peaks in according to rate, R_2
Feature Extraction		
Window before/ after selected peak	100ms	To compute baseline/ noise characteristics

Table A.2: Windows Different windows, their values and settings used in the signal processing of the eye recording data.

A.3 Parameters

Window	Value	Setting
Peak Detection and Selection		
Lambda λ	5	Multiplication factor on MAD to get peak threshold and R_1
Rate factor F	3	Multiplication factor on the obtained R_1 to get R_2
Clustering		
Sigma σ	3	A measure of spread of transformed features in during clustering

Table A.3: Parameters Different parameters, their values and settings used in the signal processing of the eye recording data.

Appendix B

Feature Selection

B.1 Using Random Forest

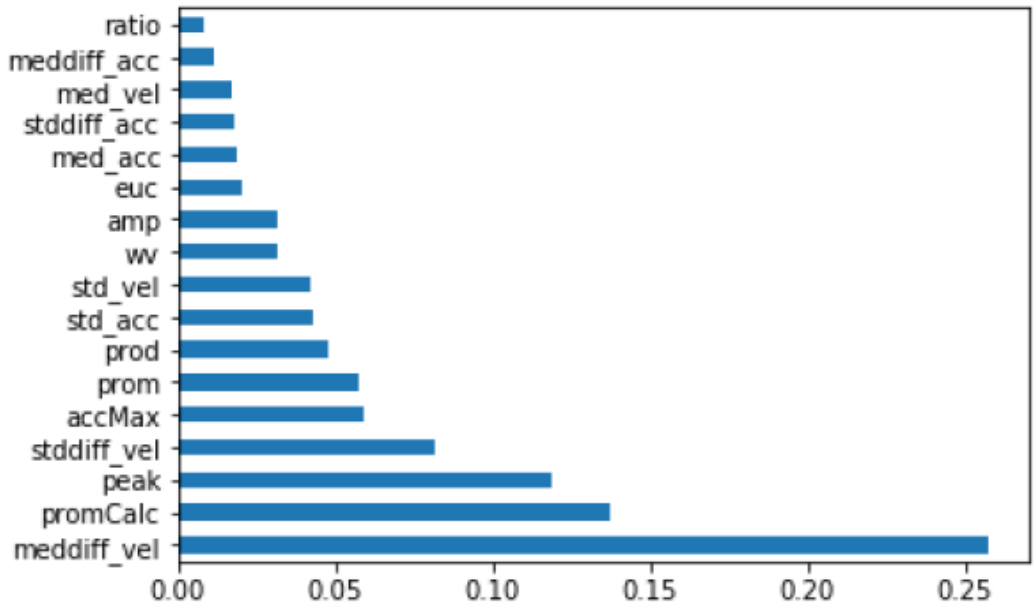

Figure B.1: Feature importance obtained using Random Forest (executed in python)

B.2 Using Spearmann's Coefficient Matrix

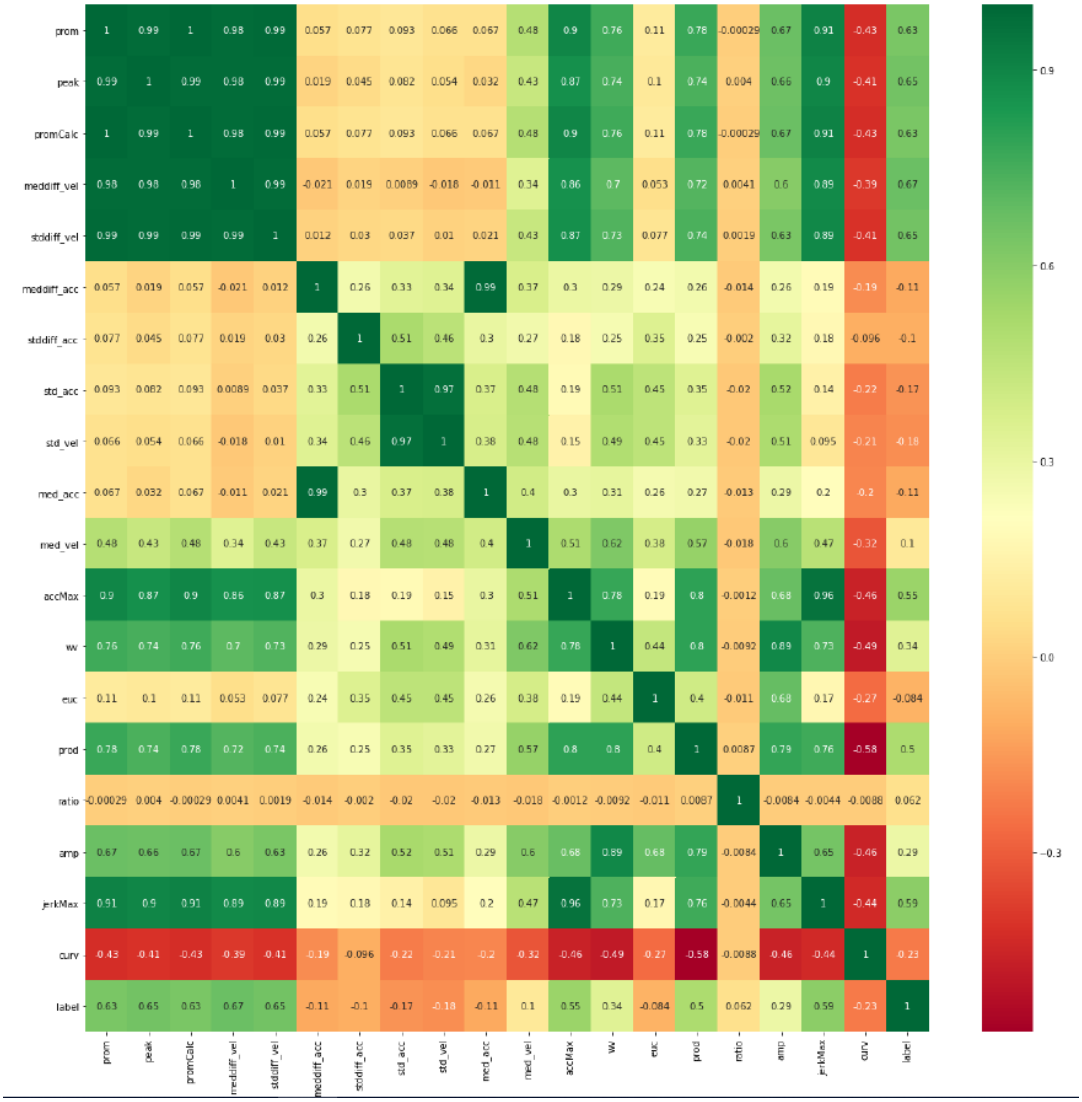

Figure B.2: Feature importance depicted using Spearmann correlation coefficient matrix

Bibliography

Abel, Larry A., Zhong I. Wang, and Louis F. Dell'Osso (2008). "Wavelet Analysis in Infantile Nystagmus Syndrome: Limitations and Abilities". en. In: *Invest. Ophthalmol. Vis. Sci.* 49.8, pp. 3413–3423. ISSN: 1552-5783. DOI: 10.1167/iovs.08-1710.

Allum, J. H. J., J. R. Tole, and A. D. Weiss (1975). "MITNYS-II-A Digital Program for On-Line Analysis of Nystagmus". In: *IEEE Transactions on Biomedical Engineering* BME-22.3, pp. 196–202. ISSN: 0018-9294. DOI: 10.1109/TBME.1975.324559.

Anantrasirichai, N., I. D. Gilchrist, and D. R. Bull (2016). "Fixation identification for low-sample-rate mobile eye trackers". In: *2016 IEEE International Conference on Image Processing (ICIP)*, pp. 3126–3130. DOI: 10.1109/ICIP.2016.7532935.

Andersson, Richard, Linnea Larsson, Kenneth Holmqvist, Martin Stridh, and Marcus Nyström (2017). "One algorithm to rule them all? An evaluation and discussion of ten eye movement event-detection algorithms". en. In: *Behavior Research Methods* 49.2, pp. 616–637. ISSN: 1554-3528. DOI: 10.3758/s13428-016-0738-9.

Arzi, M. and M. Magnin (1989). "A fuzzy set theoretical approach to automatic analysis of nystagmic eye movements". In: *IEEE Transactions on Biomedical Engineering* 36.9, pp. 954–963. ISSN: 0018-9294. DOI: 10.1109/10.35304.

Baloh, RW, Wl E Kumley, and V Honrubia (1976). "Algorithm for analyses of saccadic eye movements using a digital computer." In: *Aviation, space, and environmental medicine*.

Barnes, Graham R. (1981). *A Procedure for the Analysis of Nystagmus and Other Eye Movements.:* en. Tech. rep. Fort Belvoir, VA: Defense Technical Information Center. DOI: 10.21236/ADA112603.

Behrens, F., M. MacKeben, and W. Schröder-Preikschat (2010). "An improved algorithm for automatic detection of saccades in eye movement data and

for calculating saccade parameters". en. In: *Behavior Research Methods* 42.3, pp. 701–708. ISSN: 1554-351X, 1554-3528. DOI: 10.3758/BRM.42.3.701.

Behrens, F. and L.-R. Weiss (1992). "An algorithm separating saccadic from nonsaccadic eye movements automatically by use of the acceleration signal". en. In: *Vision Research* 32.5, pp. 889–893. ISSN: 00426989. DOI: 10.1016/0042-6989(92)90031-D.

Bell, Steven Lewis, Fiona Barker, Henry Heselton, Emma MacKenzie, Debra Dewhurst, and Alan Sanderson (2015). "A study of the relationship between the video head impulse test and air calorics". en. In: *Eur Arch Otorhinolaryngol* 272.5, pp. 1287–1294. ISSN: 0937-4477, 1434-4726. DOI: 10.1007/s00405-014-3397-4.

Bellet, Marie E., Joachim Bellet, Hendrikje Nienborg, Ziad M. Hafed, and Philipp Berens (2018). "Human-level saccade detection performance using deep neural networks". en. In: *bioRxiv*. DOI: 10.1101/359018.

Berg, David J., Susan E. Boehnke, Robert A. Marino, Douglas P. Munoz, and Laurent Itti (2009). "Free viewing of dynamic stimuli by humans and monkeys". en. In: *Journal of Vision* 9.5, pp. 19–19. ISSN: 1534-7362. DOI: 10.1167/9.5.19.

Brandt, Thomas and Michael Strupp (2005). "General vestibular testing". In: *Clinical Neurophysiology* 116.2, pp. 406–426. ISSN: 1388-2457. DOI: 10.1016/j.clinph.2004.08.009.

Brevern, M von, A Radtke, F Lezius, M Feldmann, T Ziese, T Lempert, and H Neuhauser (2006). "Epidemiology of benign paroxysmal positional vertigo: a population based study". en. In: *Journal of Neurology, Neurosurgery & Psychiatry* 78.7, pp. 710–715. ISSN: 0022-3050. DOI: 10.1136/jnnp.2006.100420.

Chang, Tzu-Pu, Adriana S. Batazzi, Jorge Otero-Millan, Joshua Betz, Zheyu Wang, Kevin A. Kerber, Jorge C. Kattah, David S. Zee, and David E. Newman-Toker (2019). "Towards an "Eye ECG" for Stroke: Artifacts in Nystagmus Velocity Measures by Video-oculography (in preparation)".

Dar, Asim H., Adina S. Wagner, and Michael Hanke (2019). *REMoDNaV: Robust Eye Movement Detection for Natural Viewing*. en. preprint. Bioinformatics. DOI: 10.1101/619254.

Daye, Pierre M. and Lance M. Optican (2014). "Saccade detection using a particle filter". In: *Journal of Neuroscience Methods* 235, pp. 157–168. ISSN: 0165-0270. DOI: 10.1016/j.jneumeth.2014.06.020.

Den Buurman, Rudy, Theo Roersema, and Jack F. Gerrissen (1981). "Eye Movements and the Perceptual Span in Reading". In: *Reading Research Quarterly* 16.2, pp. 227–235. ISSN: 0034-0553. DOI: 10.2307/747557.

Dix, M. R. and C. S. Hallpike (1952). "LXXVIII The Pathology, Symptomatology and Diagnosis of Certain Common Disorders of the Vestibular System". en. In: *Annals of Otology, Rhinology & Laryngology* 61.4, pp. 987–1016. ISSN: 0003-4894, 1943-572X. DOI: 10.1177/000348945206100403.

Dorr, Michael, Thomas Martinetz, Karl R. Gegenfurtner, and Erhardt Barth (2010). "Variability of eye movements when viewing dynamic natural scenes". en. In: *Journal of Vision* 10.10, pp. 28–28. ISSN: 1534-7362. DOI: 10.1167/10.10.28.

Eckstein, Maria K., Belén Guerra-Carrillo, Alison T. Miller Singley, and Silvia A. Bunge (2017). "Beyond eye gaze: What else can eyetracking reveal about cognition and cognitive development?" In: *Developmental Cognitive Neuroscience*. Sensitive periods across development 25, pp. 69–91. ISSN: 1878-9293. DOI: 10.1016/j.dcn.2016.11.001.

Engbert, R. and K. Mergenthaler (2006). "Microsaccades are triggered by low retinal image slip". en. In: *Proceedings of the National Academy of Sciences* 103.18, pp. 7192–7197. ISSN: 0027-8424, 1091-6490. DOI: 10.1073/pnas.0509557103.

Engbert, Ralf and Reinhold Kliegl (2003). "Microsaccades uncover the orientation of covert attention". In: *Vision Research* 43.9, pp. 1035–1045. ISSN: 0042-6989. DOI: 10.1016/S0042-6989(03)00084-1.

Engelken, Edward J and Kennith W Stevens (1989). *A New Approach to the Analysis of Nystagmus: An Application for Order-Statistic Filter*. Tech. rep. SCHOOL OF AEROSPACE MEDICINE BROOKS AFB TX.

Epley, John M. (1980). "New Dimensions of Benign Paroxysmal Positional Vertigo". en. In: *Otolaryngol Head Neck Surg* 88.5, pp. 599–605. ISSN: 0194-5998, 1097-6817. DOI: 10.1177/019459988008800514.

Erkelens, Casper J. and Olaf B. Sloot (1995). "Initial directions and landing positions of binocular saccades". en. In: *Vision Research* 35.23-24, pp. 3297–3303. ISSN: 00426989. DOI: 10.1016/0042-6989(95)00077-R.

Finkelstein, David, Josef M. Jauch, Samuel Schiminovich, and David Speiser (1962). "Foundations of Quaternion Quantum Mechanics". en. In: *Journal of Mathematical Physics* 3.2, pp. 207–220. ISSN: 0022-2488, 1089-7658. DOI: 10.1063/1.1703794.

Friedman, Lee, Ioannis Rigas, Evgeny Abdulin, and Oleg V. Komogortsev (2018). "A novel evaluation of two related and two independent algorithms

for eye movement classification during reading". en. In: *Behavior Research Methods* 50.4, pp. 1374–1397. ISSN: 1554-3528. DOI: 10.3758/s13428-018-1050-7.

Goldberg, Joseph H. and Jack C. Schryver (1995). "Eye-gaze-contingent control of the computer interface: Methodology and example for zoom detection". en. In: *Behavior Research Methods, Instruments, & Computers* 27.3, pp. 338–350. ISSN: 0743-3808, 1532-5970. DOI: 10.3758/BF03200428.

Han, Byung In, Hui Jong Oh, and Ji Soo Kim (2006). "Nystagmus while recumbent in horizontal canal benign paroxysmal positional vertigo". en. In: p. 6.

Hannaford, Philip C., Julie A. Simpson, Ann Fiona Bisset, Adrian Davis, William McKerrow, and Robert Mills (2005). "The prevalence of ear, nose and throat problems in the community: results from a national cross-sectional postal survey in Scotland". en. In: *Fam Pract* 22.3, pp. 227–233. ISSN: 0263-2136. DOI: 10.1093/fampra/cmi004.

Harezlak, Katarzyna and Pawel Kasprowski (2018). "Application of eye tracking in medicine: A survey, research issues and challenges". In: *Computerized Medical Imaging and Graphics*. Advances in Biomedical Image Processing 65, pp. 176–190. ISSN: 0895-6111. DOI: 10.1016/j.compmedimag.2017.04.006.

Hessels, Roy S., Diederick C. Niehorster, Chantal Kemner, and Ignace T. C. Hooge (2017). "Noise-robust fixation detection in eye movement data: Identification by two-means clustering (I2MC)". en. In: *Behavior Research Methods* 49.5, pp. 1802–1823. ISSN: 1554-3528. DOI: 10.3758/s13428-016-0822-1.

Hilton, Malcolm P. and Darren K. Pinder (2014). "The Epley (canalith repositioning) manoeuvre for benign paroxysmal positional vertigo". en. In: *Cochrane Database of Systematic Reviews* 12. ISSN: 1465-1858. DOI: 10.1002/14651858.CD003162.pub3.

Holmqvist, Kenneth, Marcus Nyström, Richard Andersson, Richard Dewhurst, Jarodzka Halszka, and Joost van de Weijer (2011). *Eye Tracking : A Comprehensive Guide to Methods and Measures*. English. United Kingdom: Oxford University Press. ISBN: 978-0-19-969708-3.

Hooge, Ignace T. C. and Guido Camps (2013). "Scan path entropy and arrow plots: capturing scanning behavior of multiple observers". English. In: *Front. Psychol.* 4. ISSN: 1664-1078. DOI: 10.3389/fpsyg.2013.00996.

Hoppe, Sabrina and Andreas Bulling (2016). "End-to-End Eye Movement Detection Using Convolutional Neural Networks". en. In: *arXiv:1609.02452 [cs]*.

Hosokawa, Mitsuto, Satoshi Hasebe, Hiroshi Ohtsuki, and Yozo Tsuchida (2004). "Time-Frequency Analysis of Electronystagmogram Signals in Patients with Congenital Nystagmus". en. In: *Jpn J Ophthalmol* 48.3, pp. 262–267. ISSN: 0021-5155, 1613-2246. DOI: 10.1007/s10384-003-0052-9.

Jain, Anil K. (2010). "Data clustering: 50 years beyond K-means". In: *Pattern Recognition Letters*. Award winning papers from the 19th International Conference on Pattern Recognition (ICPR) 31.8, pp. 651–666. ISSN: 0167-8655. DOI: 10.1016/j.patrec.2009.09.011.

Juhola, M. (1988). "Detection of nystagmus eye movements using a recursive digital filter". In: *IEEE Transactions on Biomedical Engineering* 35.5, pp. 389–395. ISSN: 0018-9294. DOI: 10.1109/10.1398.

Juhola, Martti, Heikki Aalto, and Timo Hirvonen (2007). "Using results of eye movement signal analysis in the neural network recognition of otoneurological patients". en. In: *Computer Methods and Programs in Biomedicine* 86.3, pp. 216–226. ISSN: 01692607. DOI: 10.1016/j.cmpb.2007.02.008.

Kasneci, Enkelejda, Gjergji Kasneci, Thomas C. Kübler, and Wolfgang Rosenstiel (2015). "Online Recognition of Fixations, Saccades, and Smooth Pursuits for Automated Analysis of Traffic Hazard Perception". en. In: *Artificial Neural Networks*. Ed. by Petia Koprinkova-Hristova, Valeri Mladenov, and Nikola K. Kasabov. Vol. 4. Cham: Springer International Publishing, pp. 411–434. ISBN: 978-3-319-09902-6 978-3-319-09903-3. DOI: 10.1007/978-3-319-09903-3_20.

Kattah Jorge C., Talkad Arun V., Wang David Z., Hsieh Yu-Hsiang, and Newman-Toker David E. (2009). "HINTS to Diagnose Stroke in the Acute Vestibular Syndrome". In: *Stroke* 40.11, pp. 3504–3510. DOI: 10.1161/STROKEAHA.109.551234.

Kim, Ji-Soo and David S. Zee (2014). "Benign Paroxysmal Positional Vertigo". In: *New England Journal of Medicine* 370.12, pp. 1138–1147. ISSN: 0028-4793. DOI: 10.1056/NEJMcp1309481.

Komogortsev, Oleg V. and Alex Karpov (2013). "Automated classification and scoring of smooth pursuit eye movements in the presence of fixations and saccades". en. In: *Behavior Research Methods* 45.1, pp. 203–215. ISSN: 1554-3528. DOI: 10.3758/s13428-012-0234-9.

Komogortsev, Oleg V, Denise V Gobert, Sampath Jayarathna, Do Hyong Koh, and Sandeep M Gowda (2010). "Standardization of Automated Analyses of Oculomotor Fixation and Saccadic Behaviors". en. In: *IEEE Trans. Biomed. Eng.* 57.11, pp. 2635–2645. ISSN: 0018-9294. DOI: 10.1109/TBME.2010.2057429.

Korda, Alexandra I., Pantelis A. Asvestas, George K. Matsopoulos, Errikos M. Ventouras, and Nikolaos Smyrnis (2018). "Automatic identification of eye movements using the largest lyapunov exponent". In: *Biomedical Signal Processing and Control* 41, pp. 10–20. ISSN: 1746-8094. DOI: 10.1016/j.bspc.2017.11.004.

Kumar, Manu, Jeff Klingner, Rohan Puranik, Terry Winograd, and Andreas Paepcke (2008). "Improving the accuracy of gaze input for interaction". en. In: *Proceedings of the 2008 symposium on Eye tracking research & applications - ETRA '08*. Savannah, Georgia: ACM Press, p. 65. ISBN: 978-1-59593-982-1. DOI: 10.1145/1344471.1344488.

Lans, Ralf van der, Michel Wedel, and Rik Pieters (2011). "Defining eye-fixation sequences across individuals and tasks: the Binocular-Individual Threshold (BIT) algorithm". en. In: *Behav Res* 43.1, pp. 239–257. ISSN: 1554-3528. DOI: 10.3758/s13428-010-0031-2.

Lanska, D. J. and B. Remler (1997). "Benign paroxysmal positioning vertigo: Classic descriptions, origins of the provocative positioning technique, and conceptual developments". en. In: *Neurology* 48.5, pp. 1167–1177. ISSN: 0028-3878, 1526-632X. DOI: 10.1212/WNL.48.5.1167.

Larsson, L., M. Nyström, and M. Stridh (2013). "Detection of Saccades and Postsaccadic Oscillations in the Presence of Smooth Pursuit". In: *IEEE Transactions on Biomedical Engineering* 60.9, pp. 2484–2493. ISSN: 0018-9294. DOI: 10.1109/TBME.2013.2258918.

Larsson, Linnéa, Marcus Nyström, Richard Andersson, and Martin Stridh (2015). "Detection of fixations and smooth pursuit movements in high-speed eye-tracking data". en. In: *Biomedical Signal Processing and Control* 18, pp. 145–152. ISSN: 17468094. DOI: 10.1016/j.bspc.2014.12.008.

Larsson, Linnéa, Andrea Schwaller, Marcus Nyström, and Martin Stridh (2016). "Head movement compensation and multi-modal event detection in eye-tracking data for unconstrained head movements". en. In: *Journal of Neuroscience Methods* 274, pp. 13–26. ISSN: 01650270. DOI: 10.1016/j.jneumeth.2016.09.005.

Lee, Sooha Park, Jeremy B Badler, and Norman I Badler (2002). "Eyes alive". In: *ACM transactions on graphics (TOG)*. Vol. 21. ACM, pp. 637–644.

Leigh, R. John and David S. Zee (2015). *The Neurology of Eye Movements*. Oxford, UK: Oxford University Press. ISBN: 978-0-19-996928-9.

Liston, Dorion B., Anton E. Krukowski, and Leland S. Stone (2013). "Saccade detection during smooth tracking". en. In: *Displays* 34.2, pp. 171–176. ISSN: 01419382. DOI: 10.1016/j.displa.2012.10.002.

Luxburg, Ulrike von (2007). "A tutorial on spectral clustering". en. In: *Stat Comput* 17.4, pp. 395–416. ISSN: 0960-3174, 1573-1375. DOI: 10.1007/s11222-007-9033-z.

Mihali, Andra, Bas van Opheusden, and Wei Ji Ma (2017). "Bayesian microsaccade detection". en. In: *Journal of Vision* 17.1, pp. 13–13. ISSN: 1534-7362. DOI: 10.1167/17.1.13.

Miura, Kenichiro, Richard W Hertle, Edmond J FitzGibbon, and Lance M Optican (2003). "Effects of tenotomy surgery on congenital nystagmus waveforms in adult patients. Part I. Wavelet spectral analysis". en. In: *Vision Research* 43.22, pp. 2345–2356. ISSN: 00426989. DOI: 10.1016/S0042-6989(03)00409-7.

Mould, Matthew S., David H. Foster, Kinjiro Amano, and John P. Oakley (2012). "A simple nonparametric method for classifying eye fixations". In: *Vision Research* 57, pp. 18–25. ISSN: 0042-6989. DOI: 10.1016/j.visres.2011.12.006.

Mulligan, Jeffrey B. (2018). "Statistical Identification of Fixations in Noisy Eye Movement Data". en. In: *Electronic Imaging* 2018.14, pp. 1–7. ISSN: 2470-1173. DOI: 10.2352/ISSN.2470-1173.2018.14.HVEI-528.

Møller, F., M. Laursen, J. Tygesen, and A. Sjølie (2002). "Binocular quantification and characterization of microsaccades". en. In: *Graefe's Arch Clin Exp Ophthalmol* 240.9, pp. 765–770. ISSN: 0721-832X, 1435-702X. DOI: 10.1007/s00417-002-0519-2.

Neuhauser, Hannelore K (2007). "Epidemiology of vertigo:" en. In: *Current Opinion in Neurology* 20.1, pp. 40–46. ISSN: 1350-7540. DOI: 10.1097/WCO.0b013e328013f432.

Neuhauser, Hannelore K., Andrea Radtke, Michael von Brevern, Franziska Lezius, Maria Feldmann, and Thomas Lempert (2008). "Burden of Dizziness and Vertigo in the Community". en. In: *Arch Intern Med* 168.19, pp. 2118–2124. ISSN: 0003-9926. DOI: 10.1001/archinte.168.19.2118.

Newman-Toker, David E. (2016). "Missed stroke in acute vertigo and dizziness: It is time for action, not debate: Missed Stroke in Acute Vertigo". en. In: *Annals of Neurology* 79.1, pp. 27–31. ISSN: 03645134. DOI: 10.1002/ana.24532.

Newman-Toker, David E., Yu-Hsiang Hsieh, Carlos A. Camargo, Andrea J. Pelletier, Gregary T. Butchy, and Jonathan A. Edlow (2008). "Spectrum of Dizziness Visits to US Emergency Departments: Cross-Sectional Analysis From a Nationally Representative Sample". In: *Mayo Clin Proc* 83.7, pp. 765–775. ISSN: 0025-6196. DOI: 10.4065/83.7.765.

Newman-Toker, DE (2014). *AVERT Phase II Trial: Acute video-oculography for vertigo in emergency rooms for rapid triage. Baltimore, MD: Johns Hopkins University; 2014.. ClinicalTrials. gov Identifier: NCT02483429*.

Ng, Andrew Y., Michael I. Jordan, and Yair Weiss (2002). "On Spectral Clustering: Analysis and an algorithm". In: *Advances in Neural Information Processing Systems 14*. Ed. by T. G. Dietterich, S. Becker, and Z. Ghahramani. MIT Press, pp. 849–856.

Nyström, Marcus and Kenneth Holmqvist (2010). "An adaptive algorithm for fixation, saccade, and glissade detection in eyetracking data". en. In: *Behavior Research Methods* 42.1, pp. 188–204. ISSN: 1554-351X, 1554-3528. DOI: 10.3758/BRM.42.1.188.

Otero-Millan, J., J. L. A. Castro, S. L. Macknik, and S. Martinez-Conde (2014). "Unsupervised clustering method to detect microsaccades". en. In: *Journal of Vision* 14.2, pp. 18–18. ISSN: 1534-7362. DOI: 10.1167/14.2.18.

Otero-Millan, Jorge, Dale C. Roberts, Adrian Lasker, David S. Zee, and Amir Kheradmand (2015). "Knowing what the brain is seeing in three dimensions: A novel, noninvasive, sensitive, accurate, and low-noise technique for measuring ocular torsion". en. In: *Journal of Vision* 15.14, pp. 11–11. ISSN: 1534-7362. DOI: 10.1167/15.14.11.

Otometrics (2018). "Insights in practice". en. In: *Insights in practice*. DOI: https://partners.natus.com/asset/resource/file/otometrics/asset/2018-03/Insights%20Special%20Collection.pdf.

Pander, Tomasz, Robert Czabański, Tomasz Przyby\la, and Dorota Pojda-Wilczek (2012). "Saccades detection in optokinetic nystagmus-a fuzzy approach". In: *Journal of Medical Informatics & Technologies* 19.

Parnes, Lorne S., Sumit K. Agrawal, and Jason Atlas (2003). "Diagnosis and management of benign paroxysmal positional vertigo (BPPV)". en. In: *CMAJ* 169.7, pp. 681–693. ISSN: 0820-3946, 1488-2329.

Pekkanen, Jami and Otto Lappi (2017). "A new and general approach to signal denoising and eye movement classification based on segmented linear regression". en. In: *Sci Rep* 7.1, p. 17726. ISSN: 2045-2322. DOI: 10.1038/s41598-017-17983-x.

Punuganti, Sai Akanksha, Jing Tian, and Jorge Otero-Millan (2019). "Automatic quick-phase detection in bedside recordings from patients with acute dizziness and nystagmus". en. In: *Proceedings of the 11th ACM Symposium on Eye Tracking Research & Applications - ETRA '19*. Denver, Colorado: ACM Press, pp. 1–3. ISBN: 978-1-4503-6709-7. DOI: 10.1145/3314111.3322873.

Ranacher, G (1977). "Nystagmus analysis by computer (author's transl)". In: *Archives of oto-rhino-laryngology* 215.3-4, pp. 257–263.

Ranjbaran, M., H. L. H. Smith, and H. L. Galiana (2016). "Automatic Classification of the Vestibulo-Ocular Reflex Nystagmus: Integration of Data Clustering and System Identification". In: *IEEE Transactions on Biomedical Engineering* 63.4, pp. 850–858. ISSN: 0018-9294. DOI: 10.1109/TBME.2015.2477038.

Reccia, R, G Roberti, and P Russo (1989). "Spectral analysis of pendular waveforms in congenital nystagmus". In: *Ophthalmic research* 21.2, pp. 83–92.

Reccia, R., G. Roberti, and P. Russo (1990). "Computer analysis of ENG spectral features from patients with congenital nystagmus". en. In: *Journal of Biomedical Engineering* 12.1, pp. 39–45. ISSN: 01415425. DOI: 10.1016/0141-5425(90)90113-2.

Rey, C. G. and H. L. Galiana (1991). "Parametric classification of segments in ocular nystagmus". In: *IEEE Transactions on Biomedical Engineering* 38.2, pp. 142–148. ISSN: 0018-9294. DOI: 10.1109/10.76379.

Roberti, G., P. Russo, and G. Segrè (1987). "Spectral analysis of electro-oculograms in the quantitative evaluation of nystagmus surgery". en. In: *Med. Biol. Eng. Comput.* 25.5, pp. 573–576. ISSN: 0140-0118, 1741-0444. DOI: 10.1007/BF02441752.

Roberts, HN, S McGuigan, B Infeld, RV Sultana, and RP Gerraty (2016). "A video-oculographic study of acute vestibular syndromes". In: *Acta Neurologica Scandinavica* 134.4, pp. 258–264.

Rodriguez, Alex and Alessandro Laio (2014). "Clustering by fast search and find of density peaks". en. In: *Science* 344.6191, pp. 1492–1496. ISSN: 0036-8075, 1095-9203. DOI: 10.1126/science.1242072.

Ross, Lynda Marie and Janet Odry Helminski (2016). "Test-retest and interrater reliability of the video head impulse test in the pediatric population". In: *Otology & Neurotology* 37.5, pp. 558–563.

Salvucci, Dario D. and Joseph H. Goldberg (2000). "Identifying fixations and saccades in eye-tracking protocols". en. In: *Proceedings of the symposium on Eye tracking research & applications - ETRA '00*. Palm Beach Gardens, Florida, United States: ACM Press, pp. 71–78. ISBN: 978-1-58113-280-9. DOI: 10.1145/355017.355028.

Santini, Thiago, Wolfgang Fuhl, Thomas Kübler, and Enkelejda Kasneci (2015). "Bayesian Identification of Fixations, Saccades, and Smooth Pursuits". en. In: *arXiv:1511.07732 [cs]*.

Sauter, D., B. J. Martin, N. Di Renzo, and C. Vomscheid (1991). "Analysis of eye tracking movements using innovations generated by a Kalman filter".

en. In: *Med. Biol. Eng. Comput.* 29.1, pp. 63–69. ISSN: 0140-0118, 1741-0444. DOI: 10.1007/BF02446297.

Sheynikhovich, Denis, Marcia Bécu, Changmin Wu, and Angelo Arleo (2018). "Unsupervised detection of microsaccades in a high-noise regime". en. In: *Journal of Vision* 18.6, pp. 19–19. ISSN: 1534-7362. DOI: 10.1167/18.6.19.

Solomon, David (2000). "Benign paroxysmal positional vertigo". en. In: *Curr Treat Options Neurol* 2.5, pp. 417–427. ISSN: 1534-3138. DOI: 10.1007/s11940-000-0040-z.

Startsev, Mikhail, Ioannis Agtzidis, and Michael Dorr (2019). "1D CNN with BLSTM for automated classification of fixations, saccades, and smooth pursuits". en. In: *Behav Res* 51.2, pp. 556–572. ISSN: 1554-3528. DOI: 10.3758/s13428-018-1144-2.

Steffen, M (1990). "A simple method for monotonic interpolation in one dimension". In: *Astronomy and Astrophysics* 239, p. 443.

Strupp, Michael and Thomas Brandt (2008). "Diagnosis and Treatment of Vertigo and Dizziness". In: *Dtsch Arztebl Int* 105.10, pp. 173–180. ISSN: 1866-0452. DOI: 10.3238/arztebl.2008.0173.

Stuart, S., B. Galna, S. Lord, L. Rochester, and A. Godfrey (2014). "Quantifying saccades while walking: Validity of a novel velocity-based algorithm for mobile eye tracking". In: *2014 36th Annual International Conference of the IEEE Engineering in Medicine and Biology Society*, pp. 5739–5742. DOI: 10.1109/EMBC.2014.6944931.

Tafaj, Enkelejda, Gjergji Kasneci, Wolfgang Rosenstiel, and Martin Bogdan (2012). "Bayesian Online Clustering of Eye Movement Data". In: *Proceedings of the Symposium on Eye Tracking Research and Applications*. ETRA '12. New York, NY, USA: ACM, pp. 285–288. ISBN: 978-1-4503-1221-9. DOI: 10.1145/2168556.2168617.

Toivanen, Miika (2016). "An advanced Kalman filter for gaze tracking signal". en. In: *Biomedical Signal Processing and Control* 25, pp. 150–158. ISSN: 17468094. DOI: 10.1016/j.bspc.2015.11.009.

Toivanen, Miika, Kati Pettersson, and Kristian Lukander (2015). "A probabilistic real-time algorithm for detecting blinks, saccades, and [U+FB01]xations from EOG data". en. In: p. 15.

Veneri, G., P. Piu, P. Federighi, F. Rosini, A. Federico, and A. Rufa (2010). "Eye fixations identification based on statistical analysis - Case study". In: *2010 2nd International Workshop on Cognitive Information Processing*, pp. 446–451. DOI: 10.1109/CIP.2010.5604221.

Veneri, Giacomo, Pietro Piu, Francesca Rosini, Pamela Federighi, Antonio Federico, and Alessandra Rufa (2011). "Automatic eye fixations identification based on analysis of variance and covariance". In: *Pattern Recognition Letters* 32.13, pp. 1588–1593. ISSN: 0167-8655. DOI: 10.1016/j.patrec.2011.06.012.

Vidal, Mélodie, Andreas Bulling, and Hans Gellersen (2012). "Detection of smooth pursuits using eye movement shape features". en. In: *Proceedings of the Symposium on Eye Tracking Research and Applications - ETRA '12*. Santa Barbara, California: ACM Press, p. 177. ISBN: 978-1-4503-1221-9. DOI: 10.1145/2168556.2168586.

Vidal, Mélodie, Ken Pfeuffer, Andreas Bulling, and Hans W. Gellersen (2013). "Pursuits: eye-based interaction with moving targets". en. In: *CHI '13 Extended Abstracts on Human Factors in Computing Systems on - CHI EA '13*. Paris, France: ACM Press, p. 3147. ISBN: 978-1-4503-1952-2. DOI: 10.1145/2468356.2479632.

Wadehn, F., T. Weber, D. J. Mack, T. Heldt, and H. Loeliger (2019). "Model-based Separation, Detection, and Classification of Eye Movements". In: *IEEE Transactions on Biomedical Engineering*, pp. 1–1. ISSN: 0018-9294. DOI: 10.1109/TBME.2019.2918986.

Wass, S. V., T. J. Smith, and M. H. Johnson (2013). "Parsing eye-tracking data of variable quality to provide accurate fixation duration estimates in infants and adults". en. In: *Behav Res* 45.1, pp. 229–250. ISSN: 1554-3528. DOI: 10.3758/s13428-012-0245-6.

Widdel, Heino (1984). "Operational Problems in Analysing Eye Movements". In: *Advances in Psychology*. Ed. by Alastair G. Gale and Frank Johnson. Vol. 22. Theoretical and Applied Aspects of Eye Movement Research. North-Holland, pp. 21–29. DOI: 10.1016/S0166-4115(08)61814-2.

Zemblys, Raimondas (2017). "Eye-movement event detection meets machine learning". In: *BioMed 2017*.

Zemblys, Raimondas, Diederick C. Niehorster, and Kenneth Holmqvist (2019). "gazeNet: End-to-end eye-movement event detection with deep neural networks". en. In: *Behav Res* 51.2, pp. 840–864. ISSN: 1554-3528. DOI: 10.3758/s13428-018-1133-5.

Zemblys, Raimondas, Diederick C. Niehorster, Oleg Komogortsev, and Kenneth Holmqvist (2018). "Using machine learning to detect events in eye-tracking data". en. In: *Behavior Research Methods* 50.1, pp. 160–181. ISSN: 1554-3528. DOI: 10.3758/s13428-017-0860-3.

Vita

Sai Akanskha Punuganti was born in Hyderabad, India in 1995. She received her undergraduate degree in Biomedical Engineering from National Institute of Technology, Rourkela in 2017. Her research interests include biomedical instrumentation and signal processing. She worked on developing a low-cost, handheld biochemical analyzer for her Bachelor's thesis, which awarded her the Institute Gold Medal for Best Undergraduate Thesis.

In 2017, Akanksha joined the Master of Science and Engineering Program in Biomedical Engineering at Johns Hopkins University. She pursued her Master's thesis in the Vestibular and Oculomotor Research Lab (VORLab), in Department of Neurology, to develop an algorithm for automatic detection of nystagmus in ED patients with dizziness and vertigo.